PL-TR-96-2292

SPACE SYSTEMS ENVIRONMENTAL INTERACTION STUDIES

M. Alvin Morgan
Alan C. Huber
David J. Sperry
A. Wallace Everest
Scott J. Moran
John O. McGarity
Marilyn R. Oberhardt
M. Paul Gough
John A. Pantazis

AMPTEK, INC.
6 De Angelo Drive
Bedford, Massachusetts 01730-2204

31 October 1996

Final Report
July 1991 — July 1996

PHILLIPS LABORATORY
Directorate of Geophysics
AIR FORCE MATERIEL COMMAND
HANSCOM AIR FORCE BASE, MA 01731-3010

This technical report has been reviewed and is approved for publication.

DAVID G. OLSON. Capt, USAF
Contract Manager
Space Plasmas and Fields Branch
Space Physics Division

MARK D. CONFER, Maj, USAF
Chief, Space Plasmas and Fields Branch
Space Physics Division

WILLIAM SWIDER
Deputy Director
Space Physics Division

This report has been reviewed by the ESC Public Affairs Office (PA) and is releasable to the National Technical Information Service (NTIS).

Qualified requestors may obtain additional copies from the Defense Technical Information Center. All others should apply to the National Technical Information Service.

If your address has changed, or if you wish to be removed from the mailing list, or if the addressee is no longer employed by your organization, please notify PL/TSI, Hanscom AFB, MA 01731-3010. This will assist us in maintaining a current mailing list.

Do not return copies of this report unless contractual obligations or notices on a specific document require that it be returned.

REPORT DOCUMENTATION PAGE

Form Approved
OMB No. 0704-0188

1. AGENCY USE ONLY (Leave blank)	2. REPORT DATE	3. REPORT TYPE AND DATES COVERED
	31 October, 1996	Final (July 1991-July 1996)

4. TITLE AND SUBTITLE

Space Systems Environmental Interaction Studies

5. FUNDING NUMBERS

PE 63410F
PR 2822 TA 01 WU AM

Contract F19628-91-C-0112

6. AUTHOR(S)

M. Alvin Morgan, A. Wallace Everest, Marilyn R. Oberhardt, Alan C. Huber, Scott J. Moran, M. Paul Gough, David J. Sperry, John O. McGarity, John A. Pantazis

7. PERFORMING ORGANIZATION NAME(S) AND ADDRESS(ES)

AMPTEK, Inc.
6 De Angelo Drive
Bedford, MA 01730

8. PERFORMING ORGANIZATION REPORT NUMBER

9. SPONSORING/MONITORING AGENCY NAME(S) AND ADDRESS(ES)

Phillips Laboratory
29 Randolph Road
Hanscom AFB, MA 01731-3010

Contract Manager: Dave Olson, Capt., USAF/GPSP

10. SPONSORING/MONITORING AGENCY REPORT NUMBER

PL-TR-96-2292

11. SUPPLEMENTARY NOTES

12a. DISTRIBUTION/AVAILABILITY STATEMENT

Approved for public release;
distribution unlimited.

12b. DISTRIBUTION CODE

13. ABSTRACT *(Maximum 200 words)*

A detailed summary of the five year effort for each of the three tasks funded under this contract is provided. Task #1 (the Photovoltaic Array Space Power Plus Diagnostics [PASP Plus] experiment effort) has been completed. Hardware was provided, spacecraft integration and test, as well as, launch and on-orbit support was rendered. With the APEX satellite's mission now at an end, all activity on this effort has ceased. A comprehensive review of the flight hardware, GSE hardware and instrument data display software developed for the mission is provided. On Task #2, hardware and software preparation for the SPREE reflight on the shuttle (TSS-1R) was carried out and on-orbit operations were supported. A preliminary summary of the wave-particle interaction findings from the returned data is presented in this report. DIDM hardware is nearing the final stage of completion. Details on the functionality of the prototype system, which has been built, is given. Under Task #3, (the Space Wave Interactions with Plasmas Experiment [SWIPE]), OEDIPUS-C hardware was delivered. Both payload integration and launch activities were supported. Initial findings from the first in-depth look at the flight data are presented.

14. SUBJECT TERMS

Photovoltaic Array Space Power Plus Diagnostics, PASP Plus; Charge Hazards and Wake Studies, CHAWS; Shuttle Potential and Return Electron Experiment, SPREE; Observation of Electric Field Distributions in Ionospheric Plasma, a Unique Solution - C, OEDIPUS-C.

15. NUMBER OF PAGES

56

16. PRICE CODE

17. SECURITY CLASSIFICATION OF REPORT	18. SECURITY CLASSIFICATION OF THIS PAGE	19. SECURITY CLASSIFICATION OF ABSTRACT	20. LIMITATION OF ABSTRACT
Unclassified	Unclassified	Unclassified	SAR

Table of Contents

Section			Page
1.	Introduction		1
2.	TASK #1 - PASP Plus Efforts		1
	2.1	Summary of Activities	2
	2.2	Review of PASP Plus Hardware	4
		2.2.1 Sun Sensor	4
		2.2.2 Langmuir Probe	5
		2.2.3 ElectroStatic Analyzer	6
		2.2.4 Transient Pulse Monitor	7
		2.2.5 Thermal Coating Calorimeter	7
		2.2.6 Quartz Crystal Microbalance	8
		2.2.7 Electron Emitter	8
	2.3	Review of PASP Plus GSE Hardware and Instrument Display Software	9
		2.3.1 GSE Hardware	9
		2.3.2 Spiderbox Display Software	10
	2.4	Instrument Data Displays	11
		2.4.1 I-V Curves <F1> Display	11
		2.4.2 Housekeeping <F2> Display	12
		2.4.3 Array Parameters <F3> Display	13
		2.4.4 Langmuir Probe <F4> Display	14
		2.4.5 ESA <F5> Display	14
		2.4.6 TPM <F6> Display	15
		2.4.7 Emitter <F7> Display	16
		2.4.8 Array Temperatures <F8> Display	17
		2.4.9 Raw Data <F10> Display	18
	2.5	GSE Historical Data Displays	19
		2.5.1 Spiderbox Database Display Screen	19
		2.5.2 ESA/LP Screen <F4> Display	20
		2.5.3 ESA Screen <F5> Display	21
		2.5.4 Bias/TPM Screen <F6> Display	22
		2.5.5 Bias/LP/Leakage Current Screen <F7> Display	23
3.	TASK #2 - CHAWS Efforts		24
	3.1	Summary of Activities	24
	3.2	DIDM Activities	25
		3.2.1 DIDM Instrument Design Overview	25
		3.2.2 Wedge & Strip Anode Design	26
		3.2.3 DIDM Analog Electronics Design	26
		3.2.4 Other Functional Elements in DIDM Analog	27
		3.2.5 DIDM Operating Modes	28
		3.2.5.1 RPA Mode	28
		3.2.5.2 Drift Meter Mode	28
		3.2.5.3 Telemetry	29

3.3 DIDM Prototype 31
3.3.1 Introduction 31
3.3.2 How the Prototype Works 31
3.3.3 Running the Software 31
3.3.4 GSE Display 32
3.3.4.1 Top Level Buttons 32
3.3.4.2 The Map Display 33
3.3.4.3 The Graph Display 35
3.3.4.4 The Control Display 35
3.3.4.5 The Hex Display 36
3.3.4.6 The FWHM Display 36
3.3.5 Hardware 37
3.4 SPREE Activities 38
3.4.1 The SPREE Instrument 38
3.4.2 MegaHertz Electron Modulations 39
3.4.3 KiloHertz Electron Modulations 40
3.4.4 Summary 42
3.4.5 References 42
4. TASK #3 - OEDIPUS-C Efforts 44
4.1 Summary of Activities 44
4.2 The OEDIPUS-C Mission 46
4.3 The Energetic Particle Instrument (EPI) 46
4.4 EPI Energy Spectra 46
4.5 Electron Heating at TX Resonances 47
4.6 Electron Responses to TX Pulses 48
4.7 Summary 49

List of Figures

Number		Page
1:	The APEX Satellite	2
2:	Langmuir Probe Sensor/Boom Assembly and Boom Footprint	5
3:	ElectroStatic Analyzer Outline Schematics	6
4:	Cross Section Schematic of QCM Sensor Head	7
5:	Cross Section Schematic of a Calorimeter	8
6:	Spiderbox Real-Time GSE Display	9
7:	Real-Time I-V Curve Display	11
8:	Real-Time Housekeeping Display	12
9:	Real-Time Array Parameters Display	13
10:	Real-Time Langmuir Probe (LP) & ElectroStatic Analyzer (ESA) Displays	14
11:	Real-Time Transient Pulse Monitor (TPM) Display	15
12:	Real-Time Emitter & ESA Monitor Voltage Displays	16
13:	Real-Time Array Temperatures Display	17
14:	Real-Time Raw Data Display	18
15:	Spiderbox Database Display Screen	19
16:	Historical ESA/LP Default Data Display	20
17:	Historical ESA/LP Zoomed-out Data Display	21
18:	Historical ESA Electron-Ion Data Display	21
19:	Historical Array Bias/LP/TPM Data Display	22
20:	Historical Array Bias/LP/Leakage /Emitter Grid Current Data Display	23
21:	Anode Detail Showing Actual Structure and Equivalent Pixel Array Map	25
22:	DIDM Analog Electronics Block Diagram	26
23:	DSP Functionality Block Diagram	27
24:	Drift Meter Mode Telemetry Structure	28
25:	Illustration of DIDM Stencil	29
26:	Default GSE Screen-Top Level Buttons & Map Display	32
27:	The Graph Display	33
28:	The Control Display	34
29:	The HEX Display	35
30:	The FWHM Display	36
31:	Block Diagram of DIDM Prototype System	37
32:	An Example Measurement Close to 90° Pitch Angle	39
33:	Occurrence of MHz Electron Modulations	39
34:	Explanation of MHz Wave Particle Interactions	39
35:	KHz Electron Modulations	40
36:	Locations in Velocity Space of Returning Electron Beams	41

37: KHz Modulation Frequencies of 25 Events 41
38: Dependence of Modulation period on FPEG pitch angle 41
39: OEDIPUS-C Launch Milestones 45
40: Synchronization of EPI Energy Steps to TX Frequency Steps 46
41: Electron Spectra for Two View Directions 47
42: Details of Electron Heating Resonances 47
43: Whole Flight Electron Heating 47
44: Electron Heating as a Function of TX Frequency 48
45: Response of Electrons to TX Pulses 48

1.0 INTRODUCTION

This is the final scientific report for Contract #F19628-91-C-0112, whose objective was to investigate spacecraft-environment interaction and space-plasma dynamics issues, especially as they relate to differential charging, discharge mechanisms, coupling between plasmas and space power systems, wake formation mechanisms, EM wave-particle interactions, and long-term radiation effects on operating systems in space.

The work was performed in three distinct *in-situ* investigatory programs (identified as Task #'s (1), (2) and (3). The efforts undertaken during the five year extent of the contract are summarized in this document. Details on the scope of the tasks, schedule milestones, experiment equipment designed and built (hardware and software), as well as, some results from the initial analysis of the returned data where available, are reported. The material is presented in serial order, with issues relating to Task #1 discussed first in Section 2.

2.0 TASK #1—PASP Plus EFFORTS

The objectives of Task #1 were accomplished in concert with the Photovoltaic Array for Space Power Plus Diagnostics (PASP Plus) program. This is a Phillips Laboratory (PL/GPSP) experiment, which was placed in orbit on the Advanced Photovoltaic and Electronics Experiment (APEX) satellite. The PASP Plus mission objectives were to: (1) measure the environmental interaction of advanced solar arrays, in relation to environmental conditions when the arrays are subjected to bias voltages up to ±500V; (2) determine the long-term radiation degradation effects on various array materials, and (3) flight qualify various array designs after an analysis of the data generated by the other two aspects of the investigation.

These objectives were to be accomplished by measuring the I-V characteristic of 16 array modules, from 12 different solar-array types, over the expected 3-year lifetime of the mission. Additionally, 10 of the 16 array modules were to be biased in voltage sequences between ±500V for a period of approximately six months to a year. Four Electric Field ($\vec{E}$) sensors and the Current Probe of a Transient Pulse Monitor (TPM) were flown to characterize the occurrence of any arc discharge during this period. The payload also included an ElectroStatic Analyzer (ESA) and a Langmuir Probe to characterize the ambient environment in terms of particle density and energy. Two Quartz Crystal Microbalances (QCM) and three Thermal Coating Calorimeters (CAL) were flown, to monitor the surface contamination exposure of the arrays and aid in tracking the magnitude of this significant factor in array performance degradation on orbit. In addition, a Dosimeter (to measure the radiation dose received at the payload) and an Electron Emitter (to vary the local plasma conditions and correspondingly widen the environmental parameters) were also flown. An illustrative sketch of APEX, which shows the location of the Payload Shelf and Deployed Payload Panel on which the contamination sensors and solar array modules are located, as well as, the Payload Module within which the other hardware items resides, is shown in Figure 1.

Amptek, Inc.'s role in the program were as follows: (1) Design and build an experiment Controller with the following constituent elements: a Central Processor unit, an Array Bias and Electrometer unit, an I-V measurement unit, a power conversion unit, and interfaces to ten instruments in the experiment's complement, as well as to the spacecraft's Payload Interface Module. (2) Provide the ESA, two QCMs, and three CALs. (3) Coordinate the integration of all the instruments onto the satellite, in cooperation with the satellite provider (Orbital Sciences Corp.) and PL/GPSP. (4) Provide Ground Support Equipment (GSE) to support spacecraft integration and test, as well as, on orbit mission operations.

2.1 Summary of Activities

Work commenced on this task during the second half of 1991, when the first steps at assembling the ESA were taken. As the instrument is a standard product for the company, it was a routine matter to assemble the unit, put it through the usual sequence of environment tests and calibrate it in both electron and ion beams in a calibration chamber. The first steps at assessing the scope of the larger task were also taken in that time period. Physical and electrical details for each of the diagnostic instruments were gathered and preliminary efforts at defining and scoping the various elements which make up the Controller were carried out. To this end, several meetings were convened with PL/GPSP personnel and others from both NASA-Lewis and Wright-Patterson AFB (these were concerned chiefly with physical layout and operation of the solar array modules specifically), as well as, with individuals from OSC, to settle on baseline interface requirements between the spacecraft and the experiment.

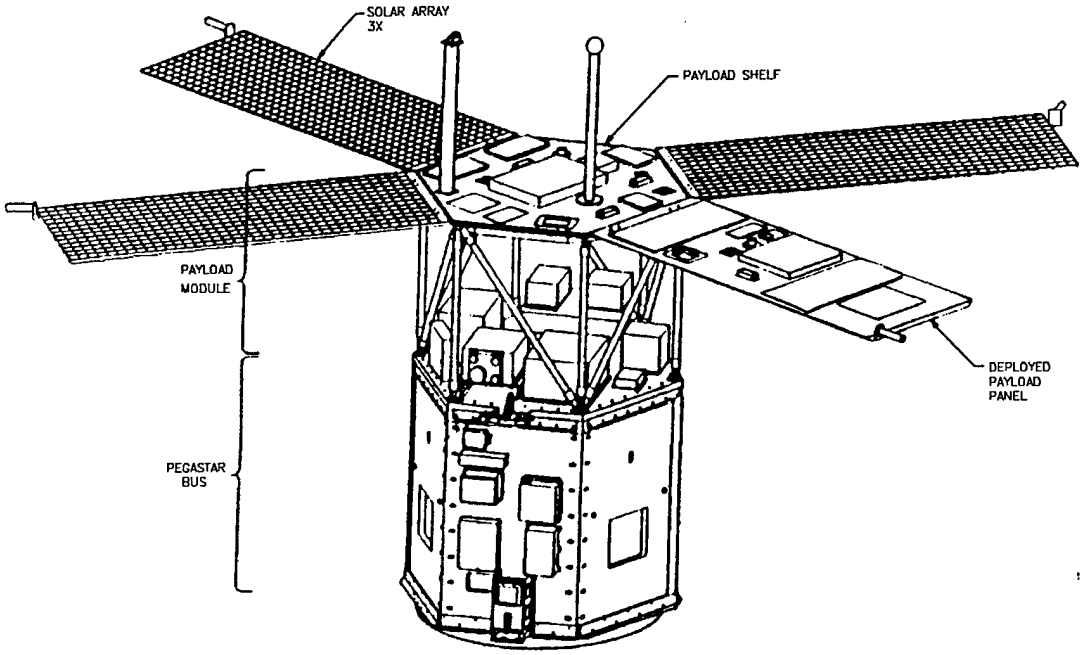

FIGURE 1: THE APEX SATELLITE

By the end of the year, the design of the various elements within the Controller were fleshed-out and fabrication of some prototype elements were underway. All of the anticipated long-lead items for the program were on order. The level of activity and the number of personnel supporting the program were increased to the maximum possible, in order to bring the necessary resources into play so that the very ambitious PASP Plus delivery to OSC, scheduled for six months hence, might be achieved. Delivery was in fact made on schedule, in the second quarter of 1992. The full, mandated sequence of environmental and functional tests were carried out prior to delivery, and although some setbacks were experienced, all proved to be surmountable and ultimately had no impact on the delivery date. Subsequently, work continued on designing and assembling GSE hardware to support on-orbit operations, and on writing software to support both real-time and post-pass mission operations activities. The principal focus of attention here was the so-called *spiderbox* hardware and software. The spiderbox was a customized PC whose tasks were to: receive the raw 128 kbits/sec APEX

downlinked telemetry; strip out the two distinct streams of PASP Plus data; port this data over a custom built local area network to a number of other data display PCs, all of whom were specifically configured with custom software to display various aspects of the returned data. This activity continued somewhat over six months after flight equipment delivery.

In parallel with this work, formal documentation matters were also attended to. The defining Command and Telemetry Allocation Document, the Interface Control Document and the various Environmental Test Reports were all delivered to PL/GPSP during this period. All work then fell into a "low level effort" status, due in-part, to integration delays on the satellite provider's end, and to short comings in contract funds to support program efforts. This state of affairs persisted for well over a year. Integration delays in particular, resulted in the delivered flight hardware being successfully integrated onto the satellite more than twelve months behind schedule. Amptek, Inc. supported PL/GPSP throughout the system integration and environmental testing processes. Various anomalous performance issues which surfaced during these exercises were addressed and resolved.

The APEX program delays fortuitously allowed much more time to work on GSE software development than was originally envisaged, and the opportunity was seized upon by PL/GPSP to make the display software in particular, a considerably more capable tool for data analysis. As a result, GSE displays ended up as a quite complex and comprehensive package, which allowed both real-time and historical downlinked data to be viewed and analyzed with ease and intuitive flexibility. A comprehensive review of the various aspects of both the realtime and historical GSE displays can be found in Scientific Report No. 3 (PL-TR-94-2215).

The preparation of GSE software (refining previously written code and the writing of new material) continued up until APEX launch, which was successfully accomplished in June 1994. Beyond the immediate period of initial experiment turn-ON and checkout, a week long period during which Company personnel were co-located with others involved with the program at the satellite control center, PASP Plus efforts were limited to providing support in trying to understand non-nominal occurrences during on-orbit operations. In general, very good data was returned by all the instruments in the PASP Plus payload and the effort put into GSE software returned rich dividends in that a very high level of data analysis was facilitated. In fact, GSE processed data was the sole means of data processing available to PL/GPSP for months after launch. All of the initially disseminated analytical information for PASP Plus was facilitated by the GSE software. Unfortunately, within a few months after orbit insertion, the satellite itself began to experience operational difficulties which significantly impaired its ability to support operational payloads.

Coincident with the implementation of a software upgrade to the Payload Interface Module on the spacecraft, which sought to "fix" an inadvertent power shut down anomaly, the PASP Plus Controller went into a non-nominal state which prevented it from functioning in a useful manner. This development occurred just a couple weeks short of the one year mark for APEX launch, and due to programmatic concerns the operational period for PASP Plus were to come to an end after twelve months anyway. Having received copious amounts of data, the quality of which exceeded all expectations, PL/GPSP declared the PASP Plus effort on APEX a success and the program ended.

2.2 Review of PASP Plus Hardware

A brief review of the hardware items in the PASP Plus payload for which Amptek, Inc. had the responsibility of either providing (design & build or procure) or integrating (Government Furnished Equipment) follows.

A total of eleven Instruments fell within Amptek Inc.'s purview for this program. They are:

1 - Sun Sensor (SS) and associated electronics.
1 - Langmuir Probe (LP) and associated electronics.
1 - ElectroStatic Analyzer (ESA).
1 - Transient Pulse Monitor (TPM) including sensors.
2 - Quartz Crystal Microbalance (QCM).
3 - Thermal Coating Calorimeter (CAL).
1 - Electron Emitter and associated electronics.
1 - Controller.

We were also tasked with providing all the necessary flight harnesses from the Controller to these instruments, as well as from the solar arrays to the Controller. The Controller, ESA, QCMs and CALs were provided by Amptek, Inc. The other instruments were supplied by PL/GPSP.

2.2.1 Sun Sensor

The Sun Sensor was flown to verify the position of the sun with respect to the Solar Array platforms. The unit is made up of a 128° x 128° field-of-view two-axis sensor head and a separate signal processing electronics module. The sun's orientation is sensed by two perpendicular photocell reticules, which generate an analog signal proportional to the intensity of the incident sunlight. The electronics module then outputs a corresponding sun angle. The unit's specifications include:

Power Requirements:	0.7 W Peak; 0.5 W NOM.
Outputs:	16-bit parallel Gray Code (8 bits per axis).
	one Intensity Threshold Output (1 bit).
Data Rate:	32 bits/sec
Sensor Size:	3.175 in x 3.175 in x 0.8 in
Sensor Weight:	0.63 lb
Electronics Size:	3.5 in x 4.5 in x 1.16 in
Electronics Weight:	0.96 lb

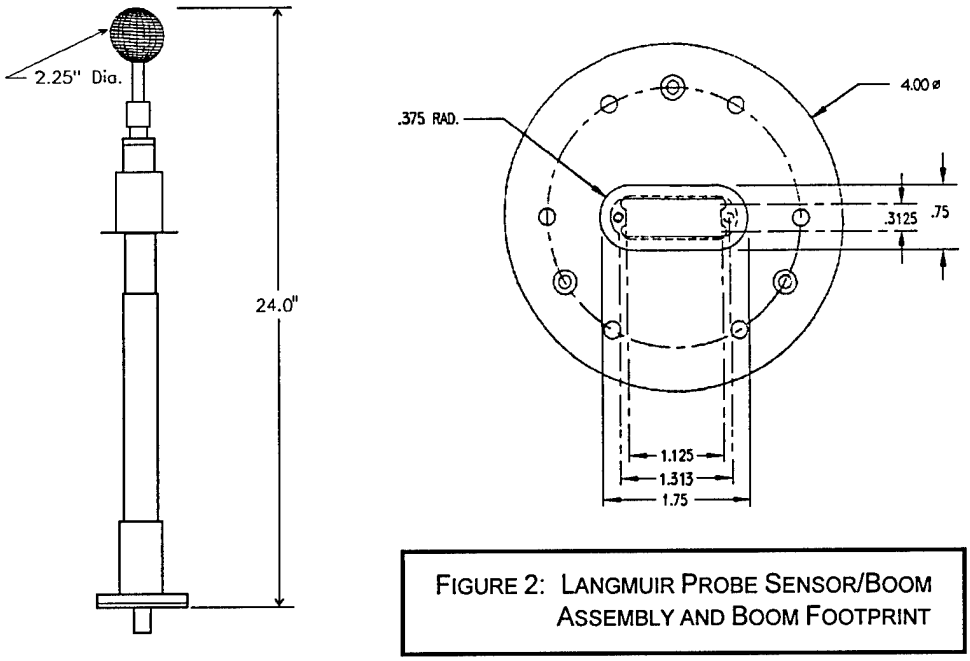

FIGURE 2: LANGMUIR PROBE SENSOR/BOOM ASSEMBLY AND BOOM FOOTPRINT

2.2.2 Langmuir Probe

The Langmuir Probe was designed to measure thermal electron density and temperature, as well as the potential of the spacecraft with respect to the ambient plasma. The unit consisted of a boom-sensor assembly (an outline of which is shown in Figure 2) and a signal processing electronics module. The Probe itself is a spherical collector surrounded by a spherical grid. The potential on the collector is swept from +4 V to -4 V with respect to the plasma and the resulting current vs. voltage characteristic is analyzed to obtain the desired information. The unit's specifications include:

Power Requirements:	3.5 W Peak; 1.6 W NOM.
Outputs:	3 Analog Signals: N_e, BIASMON, TEMPMON
Data Rate:	1152 bits/sec
Sensor Head Size:	2.25 in Dia (sphere)
Sensor Head Weight:	0.47 lb
Sensor Boom Size:	2 in Dia. (MIN) x 22 in length; 4 in Dia base
Sensor Boom Weight:	2.93 lb
Electronics Size:	7 in x 6 in x 4 in
Electronics Weight:	3.97 lb

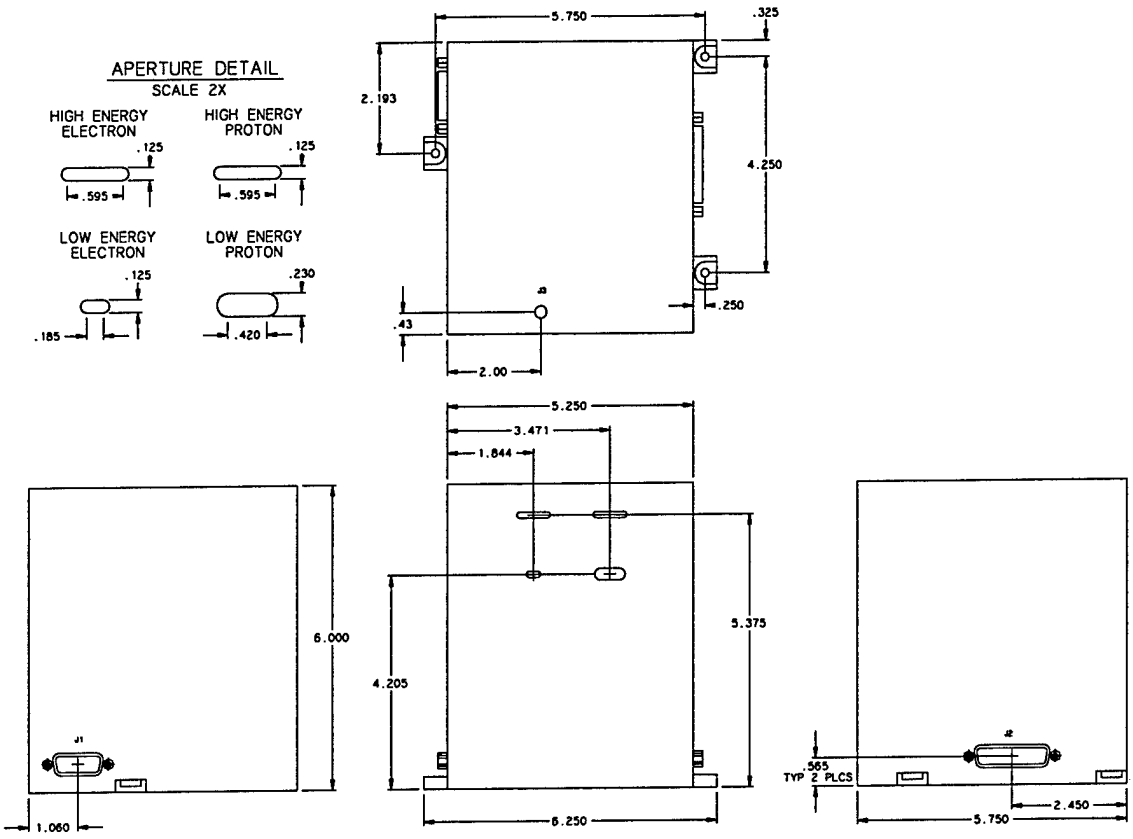

FIGURE 3: ELECTROSTATIC ANALYZER OUTLINE SCHEMATICS

2.2.3 ElectroStatic Analyzer

The ElectroStatic Analyzer was provided by Amptek Inc. and it is identical to the SSJ/4 detectors supplied to the Defense Meteorological Satellite Program (DMSP). The unit is a single module with 4 incident apertures. It measures the number of ions and electrons within the energy range of 30 eV to 30 keV, in 20 discrete channels. An outline schematic is shown in Figure 3. The units' specifications include:

Power Requirements:	0.5 W NOM.
Outputs:	4 Digital Signals: EL, EH, PL, PH
	3 Analog Signals: TEMP, HVMON, LVMON
Data Rate:	640 bits/sec for Digital Signals
	240 bits/30 sec data frame for Analogs
Dimensions:	5.75 in x 6.25 in x 6 in
Weight	4.9 lb

2.2.4 Transient Pulse Monitor

The Transient Pulse Monitor (TPM) was designed to monitor the occurrence and waveform characteristics of arc discharges from the solar arrays in the payload. The instrument determines the pulse rate, peak amplitude, rise time and pulse integral of transient electromagnetic signals, by processing the input of four Electric Field ($\vec{E}$) and one Current Probe sensors. The TPM's specifications include:

Power Requirements:	13.5 W MAX; 12.1 W NOM.
Outputs:	11 Digital Signals DATA 0 - 7, MR, SI, DR
Data Rate:	352 bits/sec
Dimensions:	
Electronics Unit	14.34 in x 8.83 in x 4.41 in
$\vec{E}$ Sensors	3.49 in x 1.30 in x 0.83 in (each)
Current Probe	2.52 in x 0.51 in x 0.51in
Weight:	
Electronics Unit	13.03 lb
$\vec{E}$ Sensors	0.19 lb (each)
Current Probe	0.19 lb

2.2.5 Thermal Coating Calorimeter

The Thermal Coating Calorimeters (three of which were flown) consist of a sensor head and a thermometer. The surface coating of each head is identical to the cover glass of a particular flight array. A change in the surface state of a unit will be reflected in a temperature change and is a direct indication of a change in the unit's ratio of absorptivity (α) to emissivity (ε). Along with the QCMs, the CALs will serve as contamination monitors for the mission. A cross-sectional schematic of a device is shown in Figure 5. The units' specifications include:

Outputs:	1 TEMP Analog Signal
Data Rate:	36 bits/30 sec data frame
Dimensions:	1.87 in x 1.87 in x 0.61 in
Weight	0.41 lb

FIGURE 4: CROSS SECTION SCHEMATIC OF A CALORIMETER

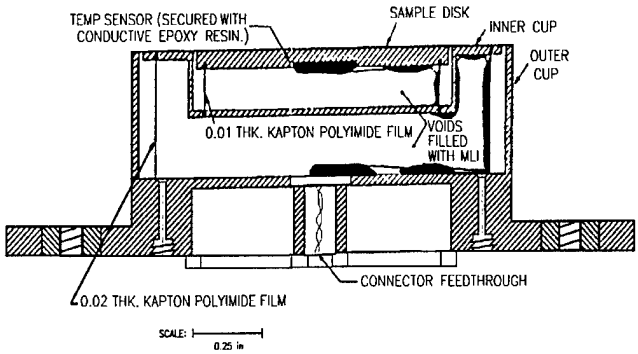

2.2.6 Quartz Crystal Microbalance

The Quartz Crystal Microbalances (two of which were flown) were designed to measure the accretion of surface contaminants on orbit. The units consist of a sensor head and a controller. The sensor head is made up of a matched pair of specially cut quartz crystals, each resonating at approximately 15 MHz. One crystal is the designated sensor, the other provides a reference signal. This signal is displaced about 1 KHz above the sensor frequency. When both signals are mixed a beat frequency results that is dependant solely on contaminant accretion. This beat frequency output is extremely sensitive: a 1 Hz shift corresponds to 1.56×10^{-9} g/cm^2 of contaminant deposition. The cross-sectional schematic of a device is shown in Figure4. The QCM's specifications include:

Power Requirements:	
Oscillators:	30 mW NOM.
Heater:	1.25 W NOM.
Outputs:	1 Digital Signal; 1 TEMP Analog Signal
Data Rate:	56 bits/30 sec data frame
Dimensions:	1.75 in Dia. x 2.42 in (each)
Weight	0.53 lb

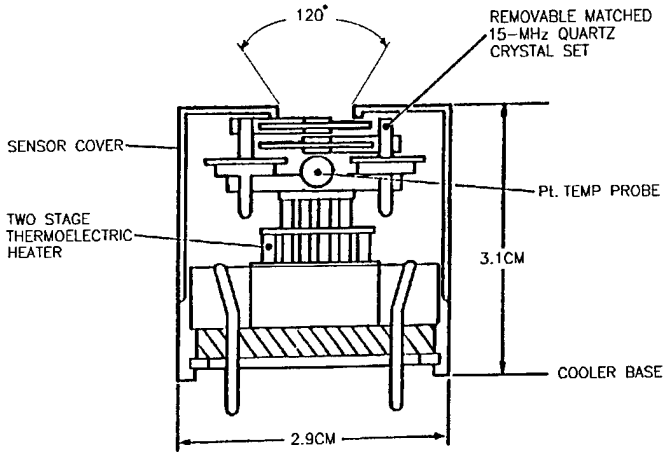

FIGURE 5: CROSS SECTION SCHEMATIC OF QCM SENSOR HEAD

2.2.7 Electron Emitter

The Electron Emitter is essentially an electron filament source which was operated for a limited period of time on orbit, in order to extend the local environmental plasma parameters and hence provide additional data points for environmental-interaction studies. It was designed and built by PL/GPSP. The unit's specifications include:

Power Requirements:	35 W NOM.
Outputs:	7 Analog Signals: Emission Mon., Bias Mon., Htr I Mon., Grid I Mon., A/B Mon, LV Mon, Temp Mon.
Data Rate:	12 bits per 30 sec Telemetry data frame for Temp Mon., 48 bits/sec total, for others
Dimensions:	8 in x 6 in x 4 in
Weight	7.14 lb (tot)

2.3 Review of PASP Plus GSE Hardware and Instrument Display Software

As was previously mentioned, the PASP Plus GSE display software was a fairly complex and comprehensive package, which allowed a great deal of ease and flexibility in viewing both the real-time and historical data downlinked from the satellite. In order to make the data available for viewing, it was necessary to design and build custom hardware, which facilitated data acquisition and extraction. Separate elements of the software ran on different processing platforms and these hardware elements were tied together in order to make data display and analysis as convenient and easy to use as possible. A brief description of the hardware elements follows in section 2.3.1 and details of the realtime display software which ran on the network server is provided in section 2.3.2. Realtime and historical payload data displays are detailed in sections 2.4 and 2.5 respectively.

2.3.1 GSE Hardware

A Local Area Network (LAN) of four IBM type PCs—one of which (referred to as the *spiderbox*) acts as a server for the others—was assembled to strip out the PASP Plus data from the APEX downlink and distribute it for viewing on the LAN PCs. Amptek, Inc. designed and built the hardware which carried out the actual data extraction. It is in the form of a printed circuit board card, which fits into a slot inside the spiderbox. APEX telemetry and a clock signal were serially fed into the spiderbox via a RS-422 synchronous link. Immediately after the clock signal is detected, on-going activities on the spiderbox are interrupted and the hardware goes into an acceptance mode for telemetered data. The nominal 128 kbits/sec input or the contingency mode's 64 kbits/sec feed (the spider-box software automatically handles either one) is examined for an identifying 4-byte synch word at the beginning of each telemetry minor frame. After this has been accomplished the contents in the frames containing PASP Plus data is retrieved and essential housekeeping information is displayed on the spiderbox display screen. Additional material is made available to a PASP Plus GSE

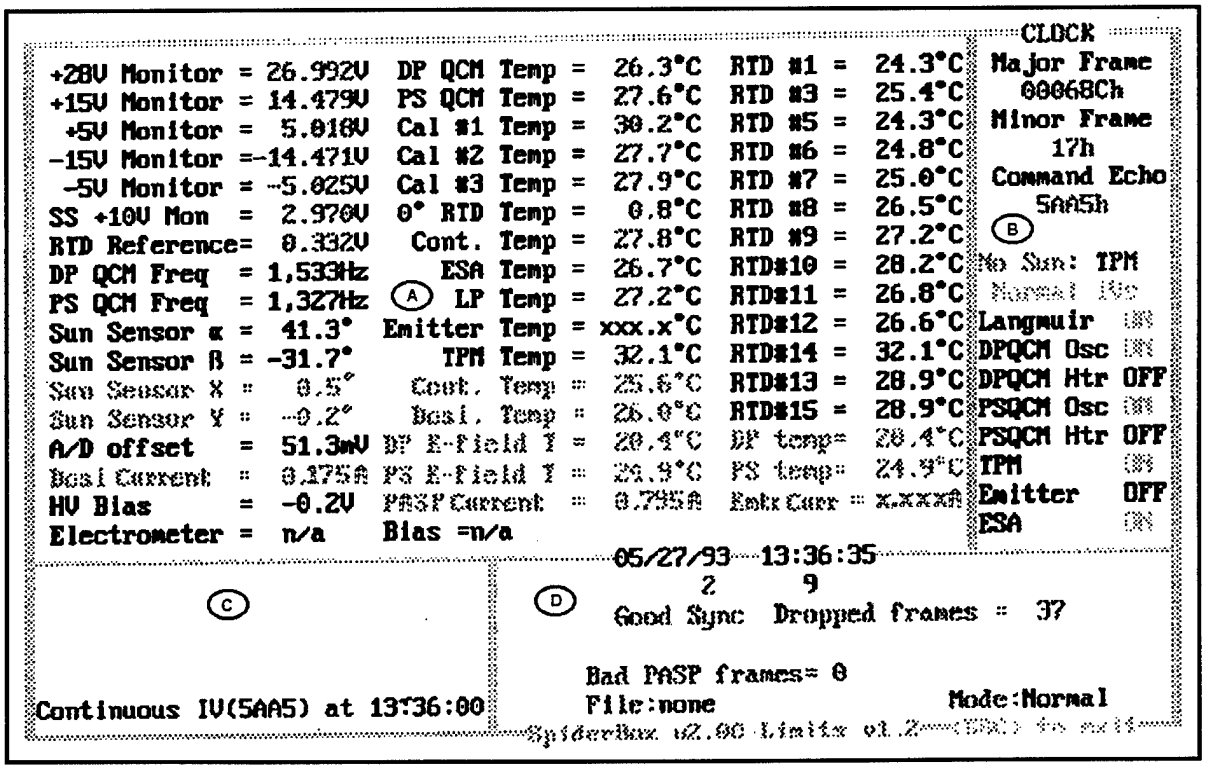

FIGURE 6: SPIDERBOX REAL-TIME GSE DISPLAY

display which shows radiation dosage information only, and to two other GSE displays on which various other instrument parameters might be observed. At the end of a downlink period, all of the telemetered data is saved in a *pass file* on the spiderbox.

2.3.2 Spiderbox Display Software

During those portions of it's orbit when APEX is in contact with the ground, essential PASP Plus instrument performance information is displayed on the spiderbox monitor in real-time. This real-time display which appears by default on the spiderbox, is shown in Figure 6. Voltage monitors for the +28V bus to the Controller and for each of the internally derived voltages are displayed in section Ⓐ. Also appearing here is the temperature of each payload unit, and of each Solar Array module which has a built-in temperature sensor. Some additional Controller calibration information (RTD Reference, A/D offset and 0° RTD Temp) are also shown here, as are the two QCM output frequencies, the PASP Plus Sun Sensor angles, the payload related temperatures which are monitored by the spacecraft, and the spacecraft's Sun Sensor output. The last two items appear among the lighter shaded entries in Figure 2 as a consequence of the fact that these parameters appear in a different color from the other entries on a color monitor, in order to easily identify them as originating from APEX and not PASP Plus system monitors. The information is stripped out of the APEX housekeeping telemetry block in the satellite downlink, and displayed with the PASP Plus derived data. The temperatures shown are those for the Deployed Panel, the Payload Shelf, the external box temperatures of the Controller, the Dosimeter and two E-Field Sensors, as well as, the APEX Sun Sensor angles.

A final inclusion in this display block are the +28V bus current for the three separate feeds to the PASP Plus payloads, i.e to the Dosimeter, the Controller and the Emitter, which are also APEX housekeeping originated data that is extracted from the downlinked telemetry for display here. This display of APEX housekeeping information is the only difference between the real-time display screen on the spiderbox and that appearing on the two principal GSE displays, GSE #1 and GSE #2. APEX acquired data is only shown on the former.

The information displayed in section Ⓑ and in section Ⓒis identical for all GSE displays. As can be seen, ON/OFF status indicators for each of the instruments in the PASP Plus payload are displayed in section Ⓑ. An indication of whether or not the sun is in view of the PASP Plus Sun Sensor, the TPM is powered and the type of the IV sampling being carried out on the array modules are also located here. At the top of the block is an indication of whether or not the telemetry clock input is running and the major and minor PASP Plus telemetry frame counters. section Ⓒ is a Command Echo block. All commands received at the Controller are displayed here, in the order received. Information which is relevant to the state of the telemetry feed is displayed in section Ⓓ. This block is unique to the Spiderbox and included in it are indications of the state of the received telemetry frames, the telemetry mode and the file to which data is being written.

2.4 Instrument Data Displays

Of the four display blocks shown in Figure 6, the particular parameters which appear in sections Ⓑ and Ⓒ remains unchanged. Different information may be displayed in section Ⓐ and in section Ⓓ however, by depressing any one of eleven function keys on the GSE #1 or GSE #2 keyboards. The specific data screen which might be so obtained, its corresponding function key and a description of the display follows.

2.4.1 I-V Curves <F1> Display

The real-time GSE I-V curve display is shown in section Ⓐ of Figure 7. It is obtained by selecting the F1 key on the keyboard. The I-V characteristic of each array module is sequentially sampled every two minutes by the PASP Plus Controller and the latest such curve is the default display (it is denoted by the word *(Auto)* next to the array number at the top of the screen) for this block. Any of the sixteen array module I-V curves may be selected for viewing however, by depressing either the plus (+) or minus (–) keys on the keyboard. This action allows the viewer to scroll through all sixteen I-V's in an incrementing or decrementing fashion.

In addition to the I-V curve, key parameters of the characteristic are also shown. These are: the open circuit voltage (Voc); short circuit current (Isc); maximum power (Pmax); array temperature and fill factor. A set of baseline numbers obtained from ground testing under simulated full sun conditions, are shown in the adjacent column for comparison purposes. It is noted too, that the payload's Sun Sensor angles appear here in this display block, as is, when biasing is being carried out an array, the biased array number, the immediate bias step voltage and the biasing conditions.

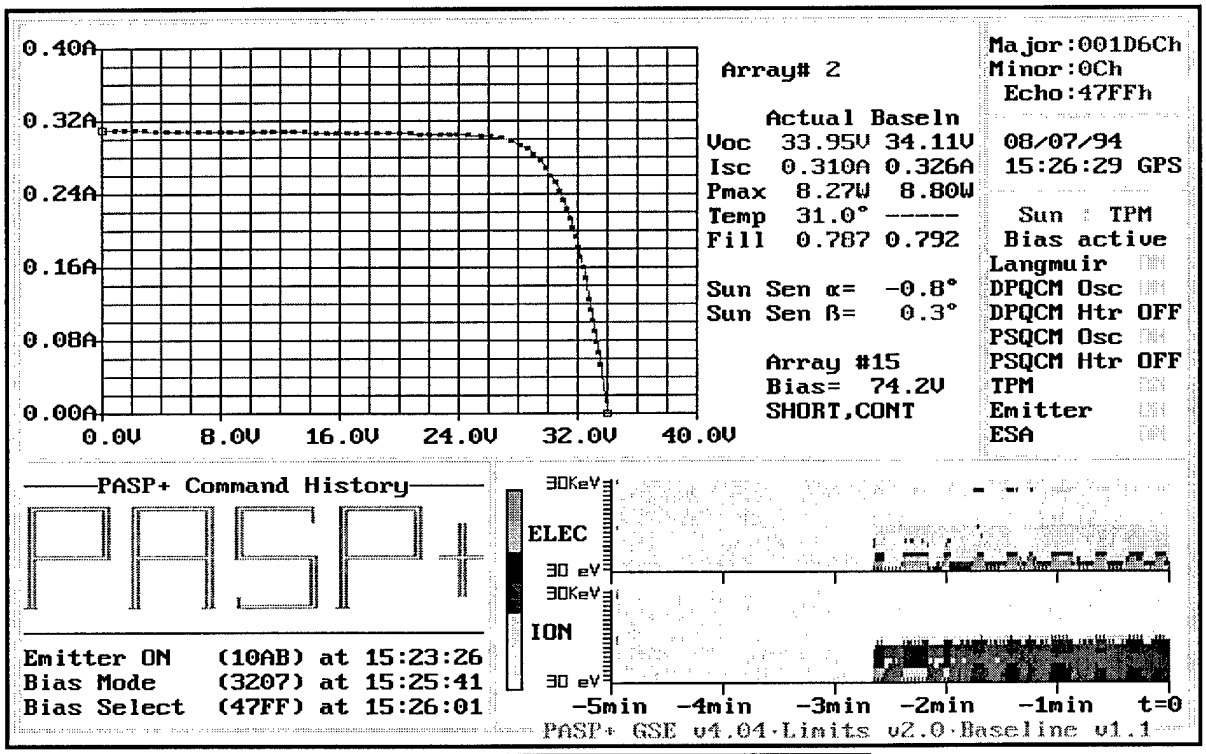

FIGURE 7: REAL-TIME I-V CURVE DISPLAY

2.4.2 Housekeeping <F2> Display

The real-time GSE housekeeping display is shown in section Ⓐ of Figure 8. It is obtained by selecting the F2 key on the keyboard. The information displayed here is almost identical to that shown in Figure 2, for the spiderbox display. The key difference is that the APEX acquired data which is stripped out of the APEX housekeeping telemetry and displayed on the spider-box, does not appear here.

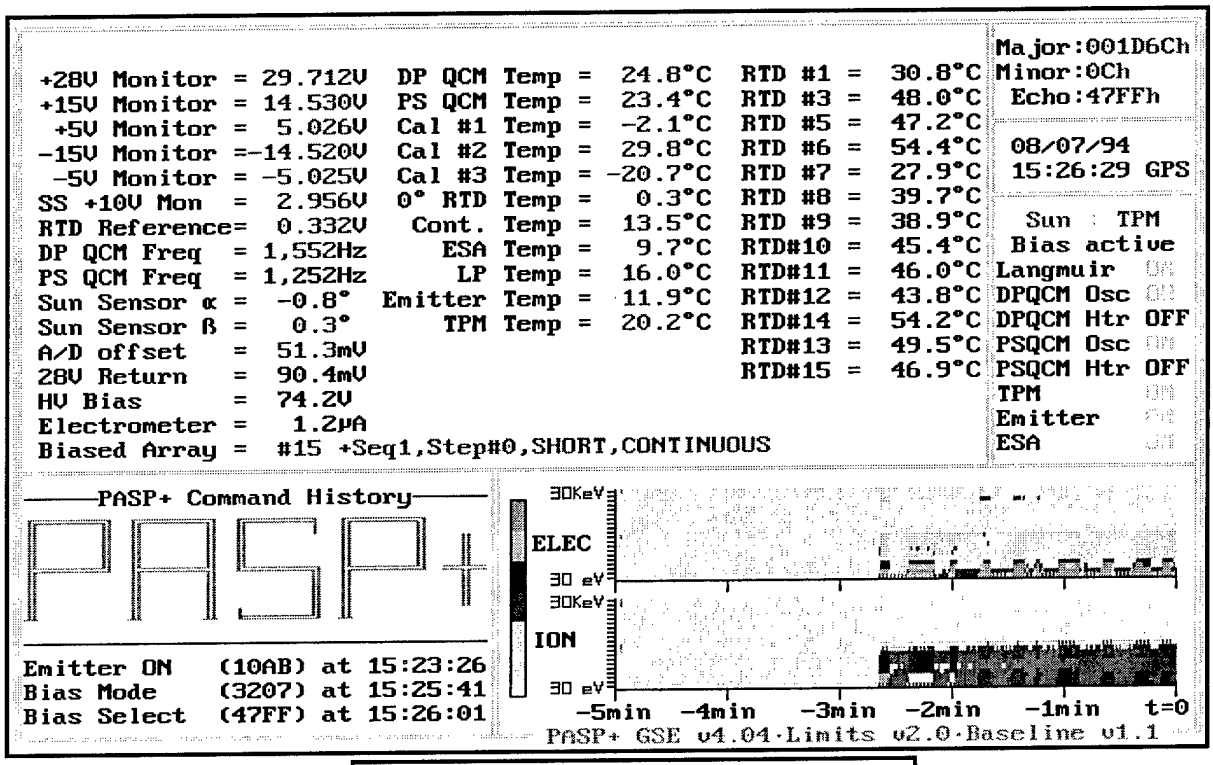

FIGURE 8: REAL-TIME HOUSEKEEPING DISPLAY

2.4.3 Array Parameters <F3> Display

The real-time GSE Array Parameters display is shown in section Ⓐ of Figure 9. It is obtained by selecting the F3 key on the keyboard. Displayed here are the key array I-V curve parameters which appear in Figure 3, for all of the Array modules. Two sets of numbers appear in the entries under each column heading. The number on the left is the measured value and it is color coded to reflect whether or not it is nominal (green), marginal (yellow) or outside the expected limits (red). The number on the right is a reference value, which was obtained from ground testing under simulated full sun conditions.

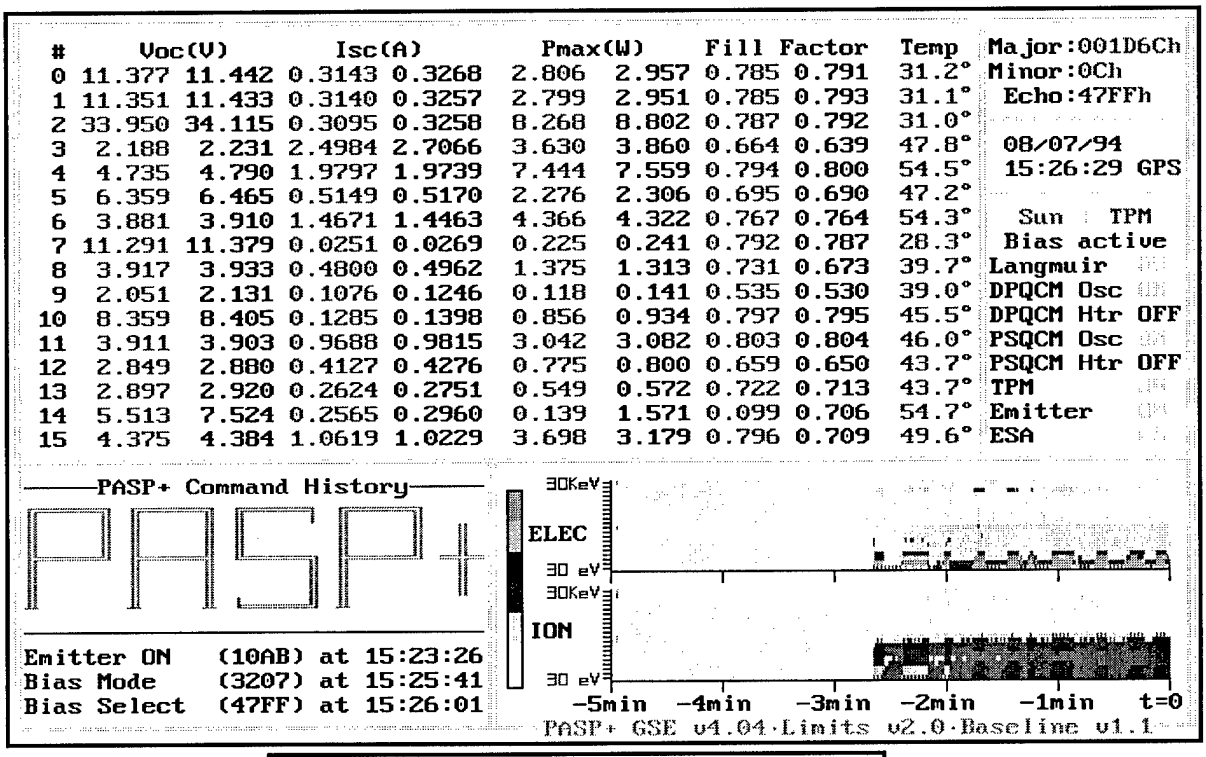

FIGURE 9: REAL-TIME ARRAY PARAMETERS DISPLAY

2.4.4 Langmuir Probe <F4> Display

The real-time GSE Langmuir Probe display is shown in section Ⓐ of Figure 10. It is obtained by selecting the F4 key on the keyboard. The information displayed here are: (i) the instrument's Ne current output plotted with the logrithmic y-axis scale on the left, and (ii) the BIASMON voltage output which is plotted with the linear y-axis scale on the right. The x-axis spans a period of one second. The instrument has within it some electronic circuitry which senses the spacecraft's potential and compensates for it, in its operation. This sensing potential (Senpot) value is shown in the middle top of the display.

2.4.5 ESA <F5> Display

The real-time GSE ElectroStatic Analyzer (ESA) display is shown in section Ⓓ of Figure 10. It is obtained by selecting the F5 key on the keyboard. Shown here is a color coded display of the output of each of the twenty energy channels, for both ions and electrons, in the instrument. The last five minutes worth of data may be observed, after which the display scrolls over. A color legend for this display block is not shown, but it is identical to that for the historical ESA data display which is forthcoming. Additional instrument diagnostic information for the ESA can be obtained with the F7 key. As will be seen shortly, voltage monitor data for both the high voltage applied to deflection plates and the low voltage used to power electronic components, are displayed here.

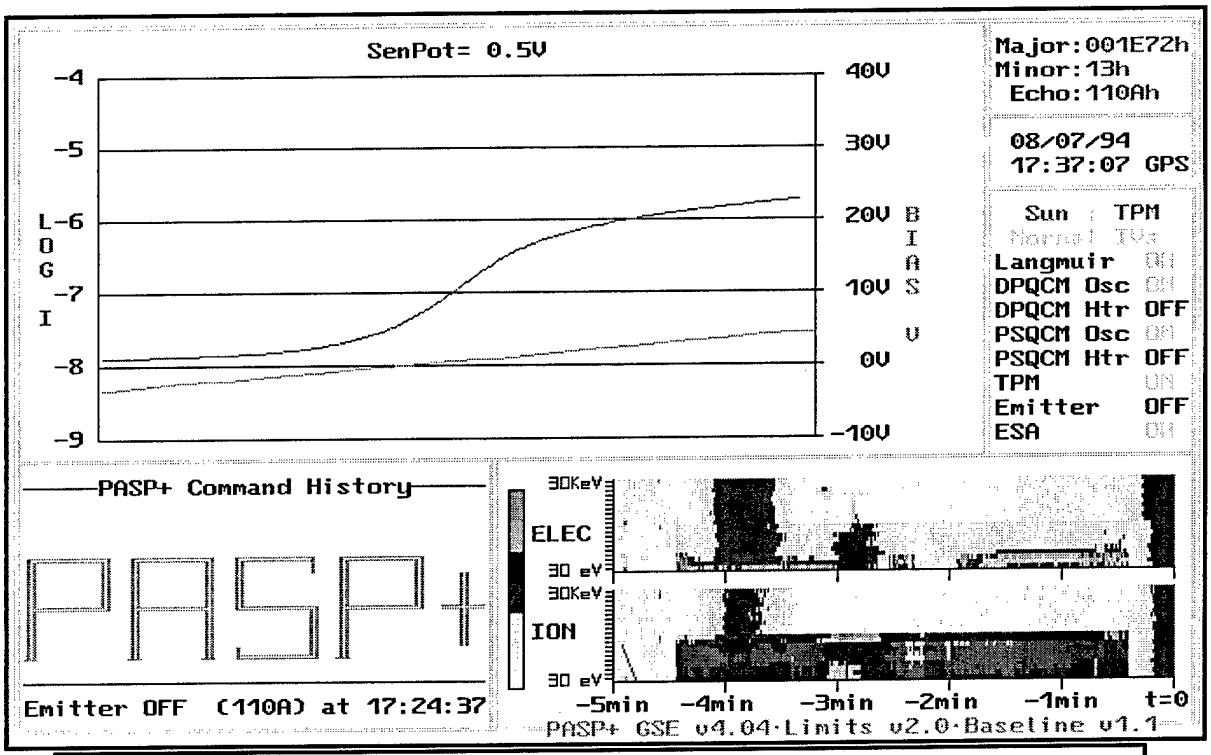

FIGURE 10: REAL-TIME LANGMUIR PROBE (LP) & ELECTROSTATIC ANALYZER (ESA) DISPLAYS

2.4.6 TPM <F6> Display

The real-time GSE Transient Pulse Monitor (TPM) display is shown in section Ⓓ of Figure 11. It is obtained by selecting the F6 key on the keyboard. This is the principal diagnostic instrument for arcing on the array modules, in response to an applied bias voltage, and its digital output is decoded and the arc characterizing data for each of its six channels is displayed here.

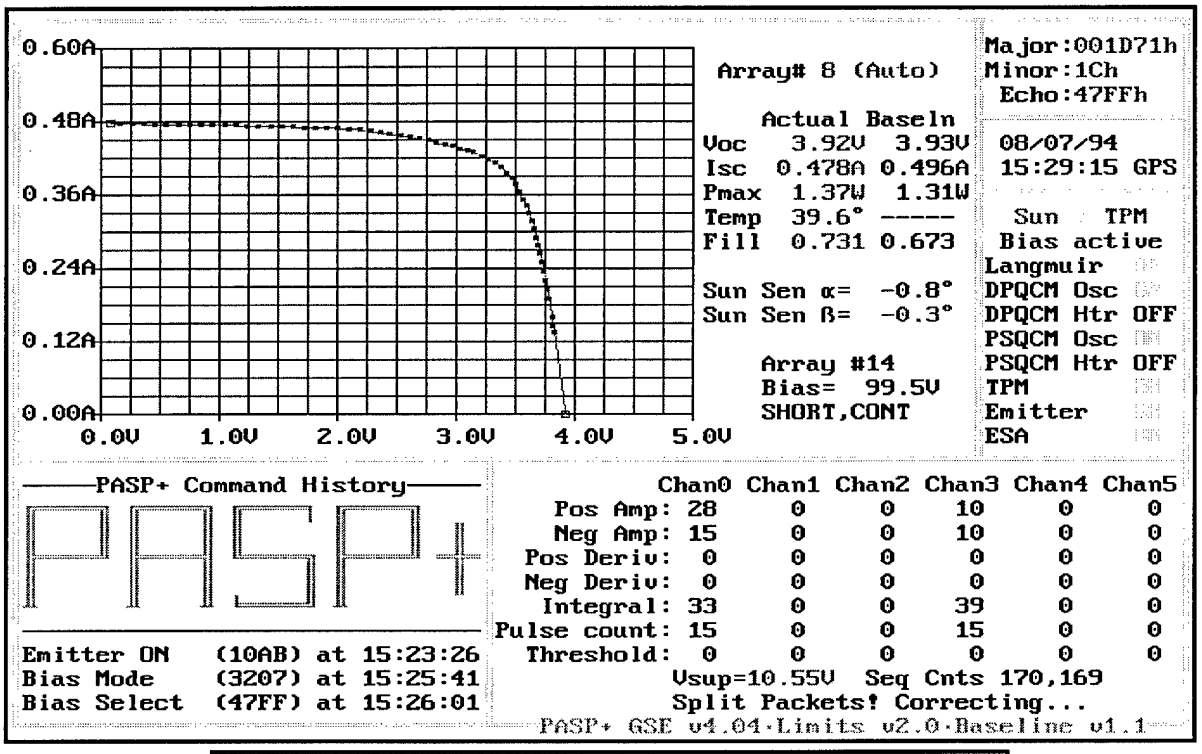

FIGURE 11: REAL-TIME TRANSIENT PULSE MONITOR (TPM) DISPLAY

2.4.7 Emitter <F7> Display

The real-time GSE Emitter display is shown in section Ⓓ of Figure 12. It is obtained by selecting the F7 key on the keyboard. The first six entries in this display block provide diagnostic information about the state of the instrument and its performance. The other entries are performance data for the ESA.

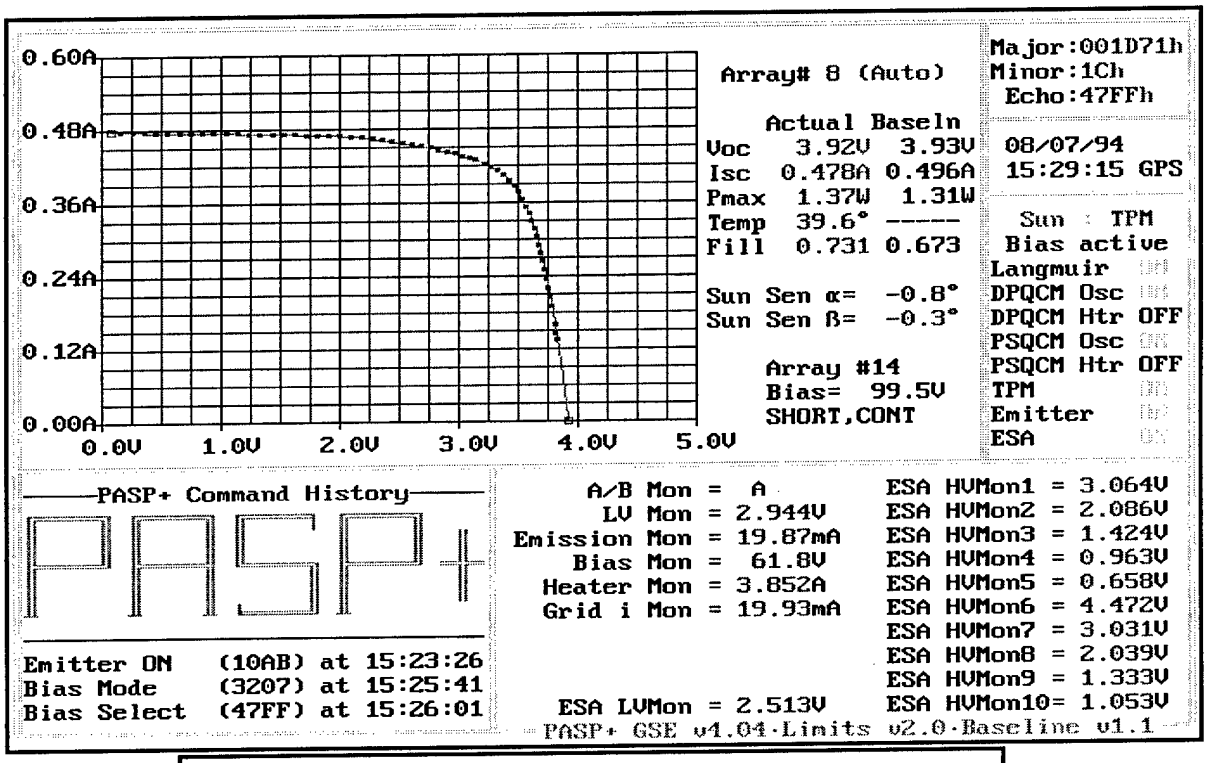

FIGURE 12: REAL-TIME EMITTER & ESA MONITOR VOLTAGE DISPLAYS

2.4.8 Array Temperatures <F8> Display

The real-time GSE array temperature display is shown in section Ⓐ of Figure 13. It is obtained by selecting the F8 key on the keyboard. The temperature of each array module with a built-in temperature sensor or RTD on the Deployed Panel, is shown in a distinguishing color on this screen for a time period of up to three hours. This function key toggles, so that by pressing it a second time the temperature for the modules on the Payload Shelf can be observed.

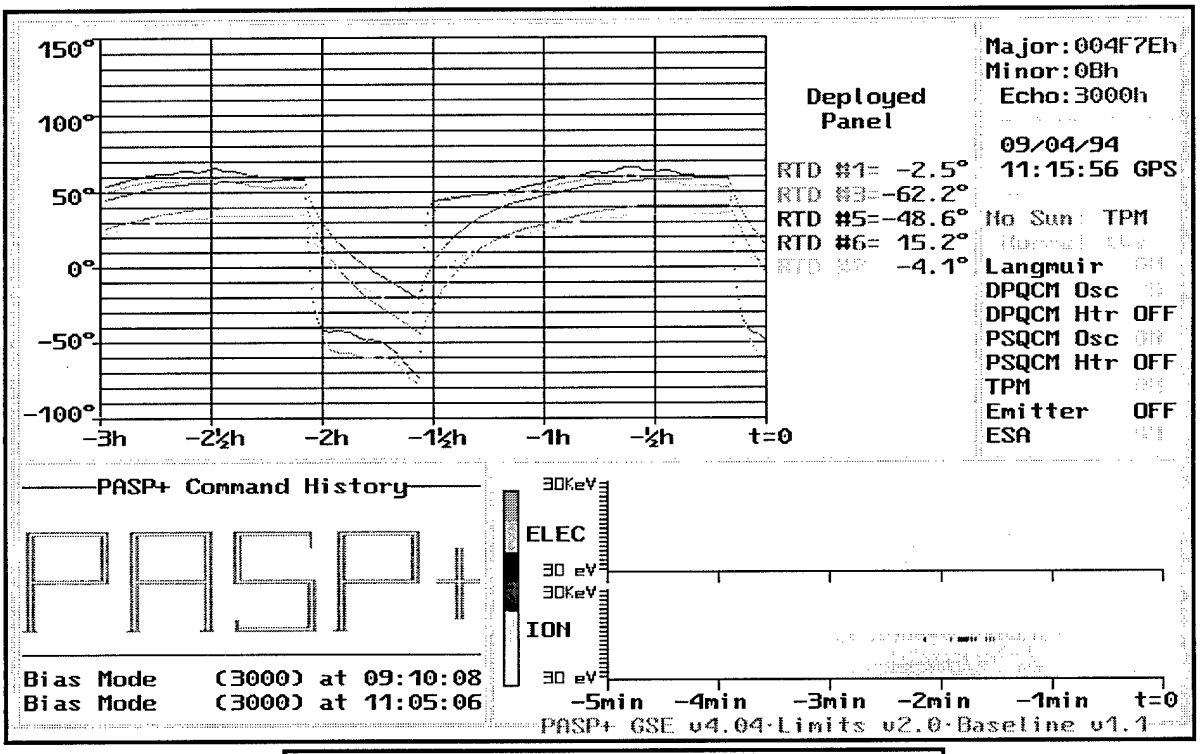

FIGURE 13: REAL-TIME ARRAY TEMPERATURES DISPLAY

2.4.9 Raw Data <F10> Display

The real-time raw data display is shown in section Ⓐ of Figure 14. It is obtained by selecting the F10 key on the keyboard. The 256 bytes returned by the Controller each second can be seen in this display, in hexadecimal format. It is this data that is decommed and shown in all of the other displays and it is sometimes useful, to revert back to this comprehensive source to observe particular aspects of the data, to compare changes in specific byte blocks that are not otherwise observable, or even to double-check the authenticity of the data elsewhere.

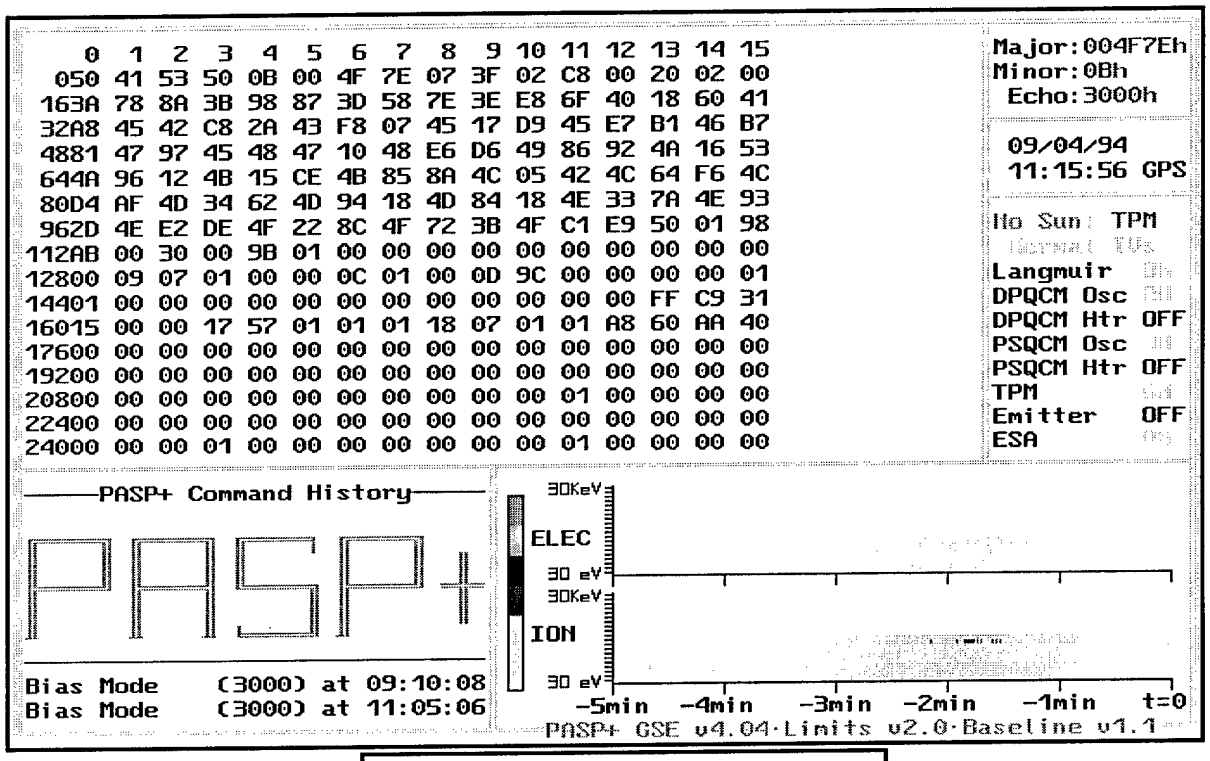

FIGURE 14: REAL-TIME RAW DATA DISPLAY

2.5 GSE Historical Data Displays

2.5.1 Spiderbox Database Display Screen

Figure 15 shows the default Spiderbox screen at the end of a satellite contact period. It is essentially a file allocation table with PASP Plus data file entries which were created from each contact download. The data filename, as well as, the beginning and end period over which the data was acquired on-orbit are the fist items displayed. An indication of whether or not any of the five payload units which can be turned ON/OFF by ground command—i.e. the Langmuir Probe (LP), Emitter (EM) Transient Pulse Monitor (TPM) and the ElectroStatic Analyzer (ESA)—was turned ON within a file, is also shown, in addition to whether or not array biasing (BIAS), arcing (HVR), or continuos I-V (CIV) sampling, occurred. The final entry shows the number of commands executed by the Controller during the duration of the file.

Immediately after the Spiderbox screen display reverts to the default shown in Figure 15, it transfers a copy of the latest data file to the root directory of each PC connected to the LAN. The GSE program *PASPOF.EXE* which is installed on the network, can then be used to look at specific features of the data in this or any other file in the Spiderbox database.

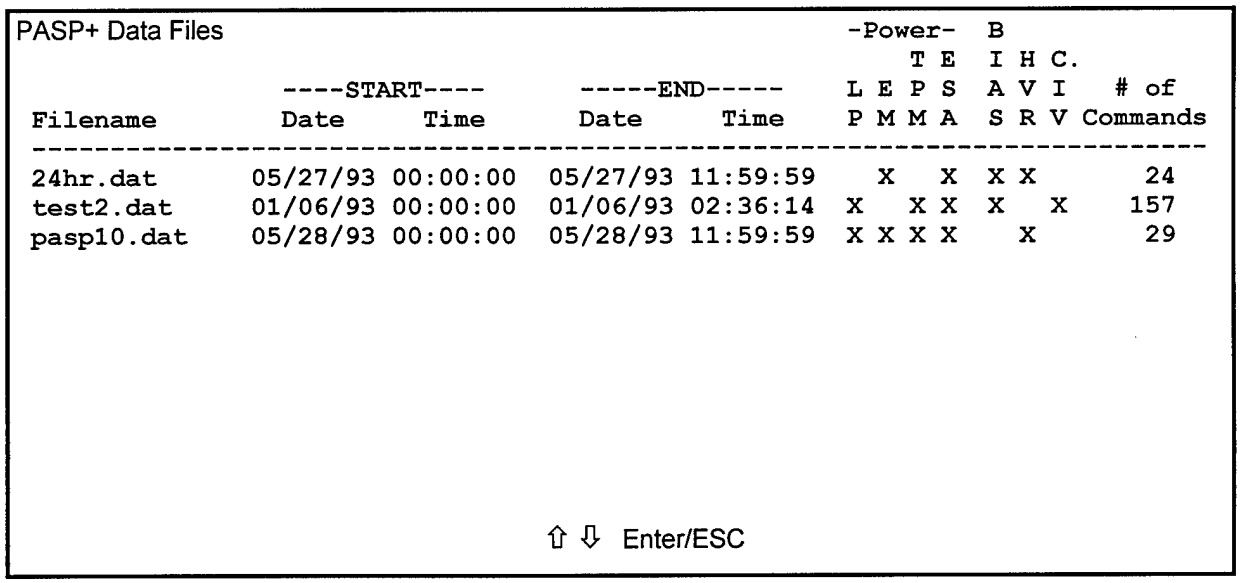

FIGURE 15: SPIDERBOX DATABASE DISPLAY SCREEN

2.5.2 ESA/LP Screen <F4> Display

An illustration of the ESA Electrons/LP Electron Density display screen showing on-orbit data is presented in Figure 16. On selecting the ESA/LP Screen <F4> for display, the program automatically looks through the file for the first occurrence of ESA and LP data and displays the initial four minutes worth. By pressing either the plus (+) or minus (-) keys the display toggles with another zoomed-out view, in which up to three hours worth of data is shown. An illustration of this is shown in Figure 17. Both figures show the counts from the ESA's electron channel (twenty of them ranging in energy from 30eV to 30keV) in the upper display, and the electron density as calculated from the Languir Probe's Ne output in the lower view. The time appearing on the x-axis is derived from the GPS time-tag associated with PASP Plus data, as recorded by APEX and telemetered with each download. The Spiderbox software extracts this information and makes it available in coordinated fashion, with the rest of the data. This is done for all of the historical data displays. Additional features which are common to all are: (a) an indication of whether of not the sun is in view of the PASP Plus Sun Sensor, and (b) the ON/OFF status of the Emitter. These appears at the top of the display. (c) Also, from an Options menu at the bottom of each screen there is provision to begin viewing the contents of a data file from its beginning <F1>, to go to a specific timetag <F2>, to scroll forward or backwards in the data file <←/→>, as well as, to zoom out to a longer display period <+/->. It is also possible to print the current screen <F11>, or to select other instrument screen displays. Additional displays are available for: (i) ESA data, in the form of a combination electron-ion spectral display <F5>; (ii) Bias/TPM data <F6>; (iii) and a combination Bias/Leakage Current/LP data <F7>,.

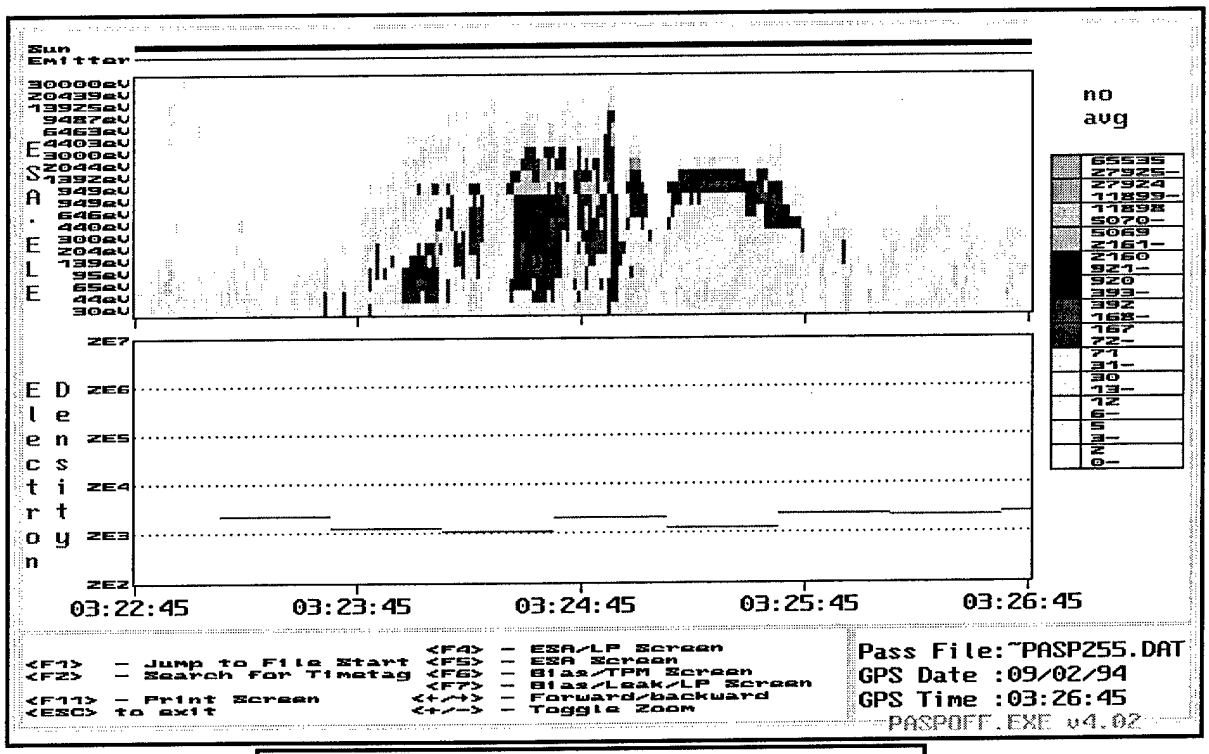

FIGURE 16: HISTORICAL ESA/LP DEFAULT DATA DISPLAY

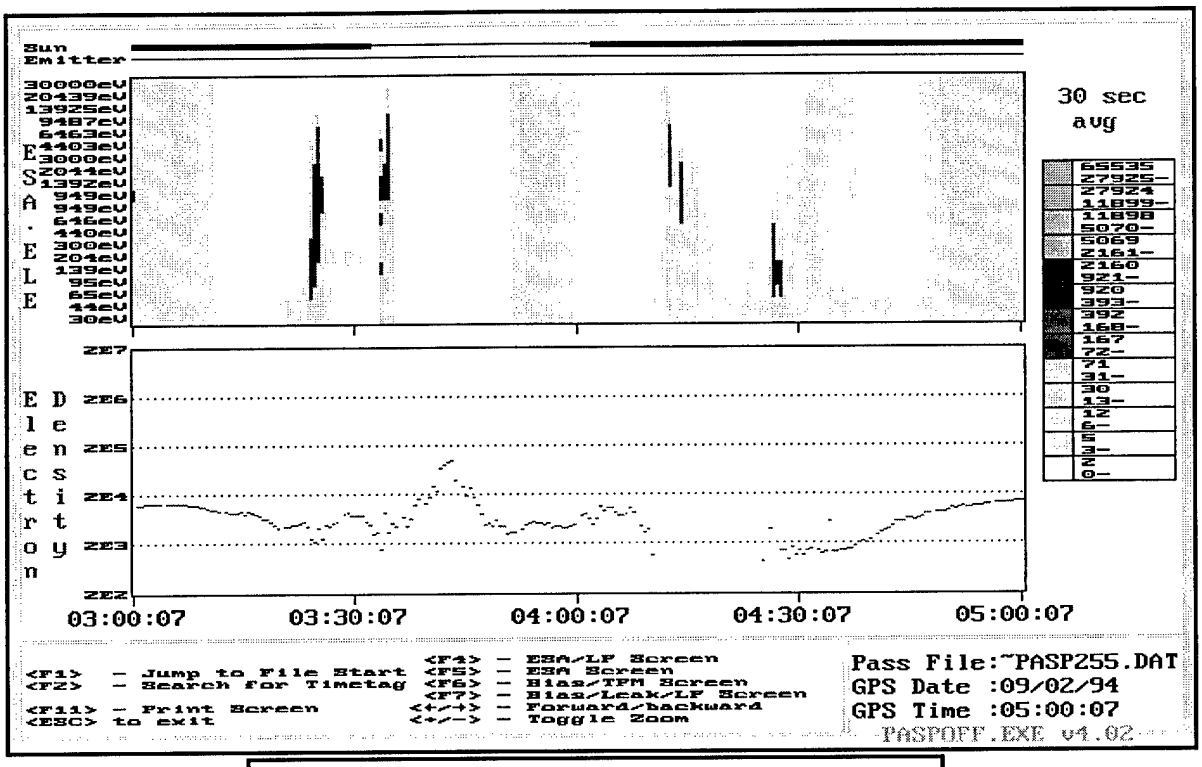

FIGURE 17: HISTORICAL ESA/LP ZOOMED-OUT DATA DISPLAY

2.5.3 ESA Screen <F5> Display

The ESA displays are illustrated in Figure 18. Here, the spectra for both ions and electrons is shown on the same time-base, in a color coded display. All twenty discrete instrument channels, within the energy range of 30 eV to 30 keV, are represented for both particle species..

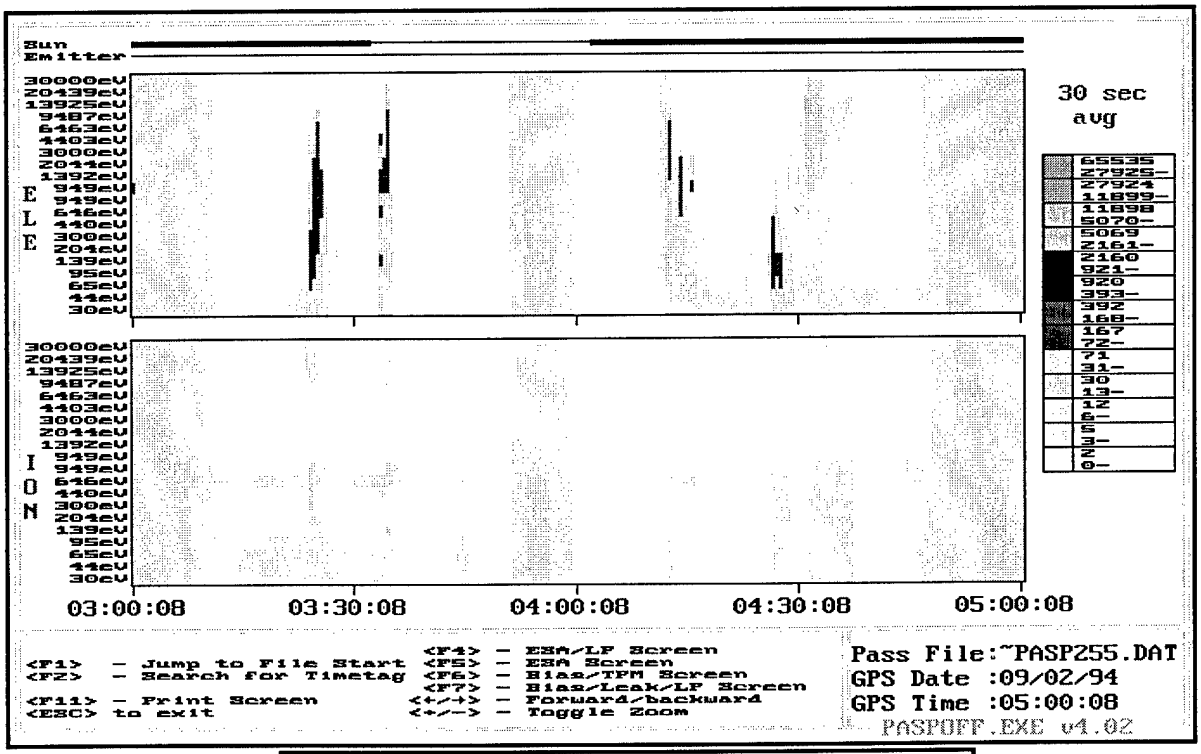

FIGURE 18: HISTORICAL ESA ELECTRON-ION DATA DISPLAY

2.5.4 Bias/TPM Screen <F6> Display

The Array Bias/LP/TPM display is shown in Figure 19. It shows at a glance the biasing particulars on the solar array modules, and the TPM's response to that activity. The module number to which bias voltage is applied, as well as the magnitude and duration of the bias, are shown in the display panel at the top of the screen. Both positive and negative voltage steps are accommodated for values between -500V to +500V. Any discontinuity in the biasing profile will be displayed, including those resulting from high voltage resets due to arcing, or APEX late polling timeouts. It is possible to distinguish on a color monitor, which of these events occurred and when it happened. Although it is difficult to see in Figure 15, the electron density—as determined from the Langmuit Probe's Ne output—is also overlaid on this display. The y-axis scale on the left hand side of the screen gives is used to determine the actual number density.

Data on a specific array module can be called up for display by selecting <F3> on the keyboard. In this instance, only data for the chosen array will be shown. The default display—as is seen in Figure 19—is to display the first available modules that fit within the x-axis timeframe.

The TPM output appears in the panel immediately below that for the array Bias and Langmuir Probe, in the bottom half of the screen. It is a compact display which shows the three principal TPM output parameters at a glance. A count of the number of events recorded for each of the five E field sensor channel (CNT 0..5) is shown in the top half of the panel, and the peak amplitude for both positive and negative discharges (AMP 0..5) in each channel, is shown in the lower half. A color legend for both counts and amplitude is shown to the right of the panel and although it is not apparent in Figure 19, negative and positive amplitudes of the same magnitude are differentiated in color, by a specific fill pattern.

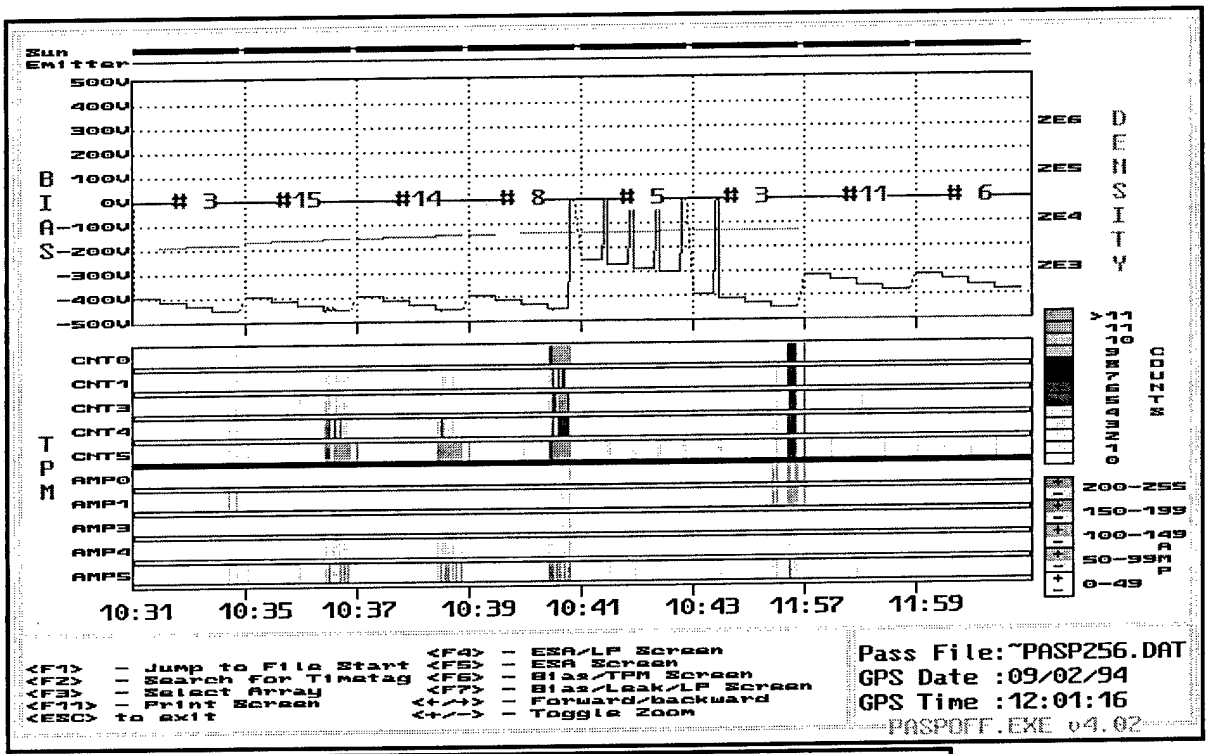

FIGURE 19: HISTORICAL ARRAY BIAS/LP/TPM DATA DISPLAY

2.5.5 Bias/LP/Leakage Current Screen <F7> Display

The final historical data display screen is the array Bias/LP/Leakage/Emitter Grid Current display shown in Figure 20. It is obtained by selecting the F7 function key. The display reflects the need to see at a glance, all of the key parameters necessary to make bias step determination decisions, when real-time array biasing is underway. Hence, the Bias Step information superimposed with the LP electron density data from Figure 15, is replicated in the top panel of the display panel. In the bottom panel, leakage current is superimposed on emitter grid current for the display. Leakage Current is most meaningful when an array module is being positively biased, and the Emitter Grid Current is necessarily only present when the Emitter is powered ON.

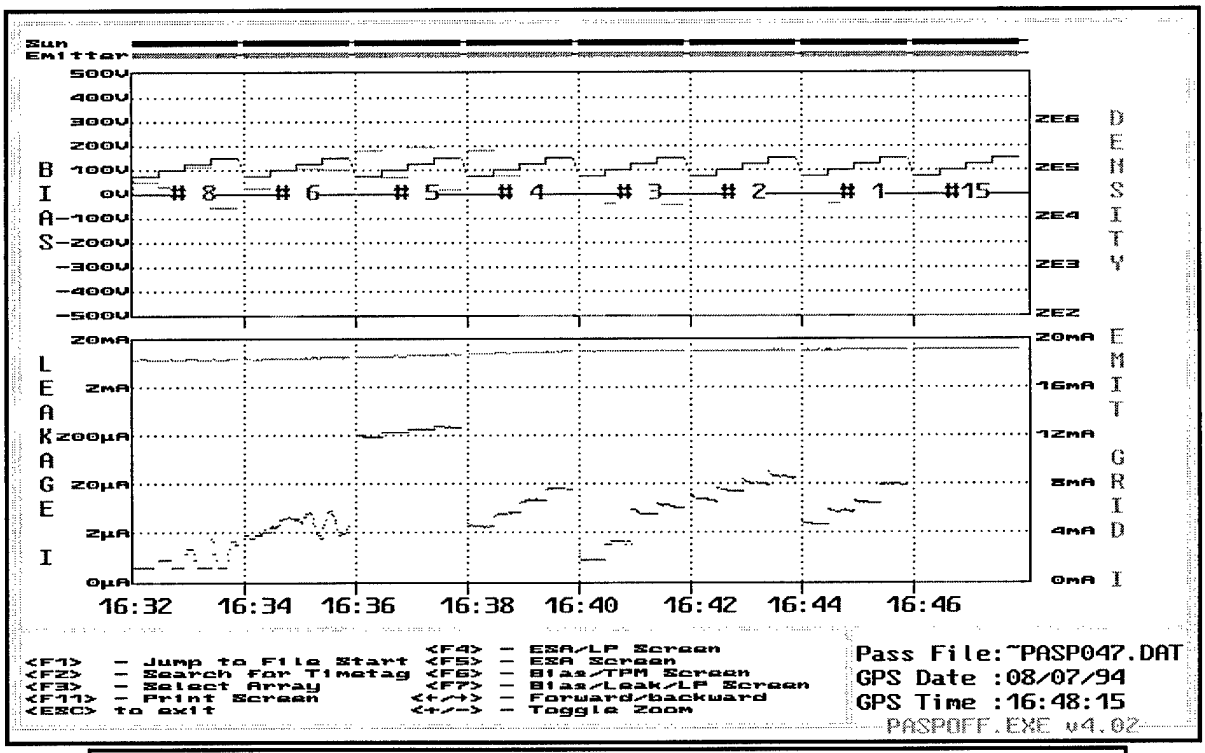

FIGURE 20: HISTORICAL ARRAY BIAS/LP/LEAKAGE /EMITTER GRID CURRENT DATA DISPLAY

3.0 TASK #2—CHAWS EFFORTS

3.1 Summary of Activities

The objectives of Task #2 were originally to be accomplished in the Charge Analysis and Wake Studies (CHAWS) portion of the Wake Shield Facility (WSF) Program. The program is a shuttle launched one, and is dedicated to material processing investigations in the near zero gavity environment of low earth orbit. The mission objectives for CHAWS were as follows: (1) to study the physics of wake formation in the ionosphere. (2) to study the process of object charging in wakes and (1) to develop new thermal space plasma diagnostics for particle densities on the order of 1 per cm^3. The principal diagnostic tool was a set of novel Retarding Potential Analyzers RPAs) which were developed for the mission. Amptek, Inc. provided technical support to the design and development effort of the RPAs. The company also designed and built the a High Voltage Power Supply (HVPS) module for one of the instruments in the CHAWS diagnostic suite. Much of this work was completed by the end of 1991. The HVPS was delivered in the first quarter of 1992, along with some additional hardware components for CHAWS which were supplied by the company.

Further hardware and consultative support was rendered to PL/GPSP over the next twelve months as the payload was first assembled and tested, and then as it made its way through the shuttle system integration and test processes. As these activities gradually came to an end. The focus of this task shifted to refining a key element in one of the instruments. This so-called "wedge an strip" anode is the key sensing element in one of the RPAs developed for the mission. It is capable of spatially resolving the entrance angle of an incident particle two-dimensionally, in cylindrical coordinates. The first effort was fairly crude, in that only a 90° resolution was possible. Amptek, Inc. was tasked with reducing this to 3°.

The anode was redesigned and several attempts at fabricating the new piece were made over the course of the next year. This objective was ultimately achieved, but after rigorously scrutinizing its electrical performance, it was determined that additional refinements would have to be made to the fabrication process in order to make the device usable. Specifically, it was found necessary to have a thin coating of Gold (≈ 1000 Å) over the Chromium surface of the device, in order to reduce the intrinsic resistivity to usable levels. In the second quarter of 1994, a meeting was convened at PL/GPSG to discuss a flight opportunity for an instrument incorporating the anode. A new instrument, designated as the Digital Ion Drift Meter (DIDM) was earmarked to receive the device and Amptek, Inc. was tasked with designing and providing the necessary electronics for a functional instrument, as well as, with producing the desired anodes for the instrument's sensors. It was agreed that PL/GPSG would retain responsibility for the manufacture and assembly of the mechanical elements of the sensors.

In the third quarter, the terms of reference for this task in the original technical proposal was amended as to: *Investigate the relationship of ambient parameters to particle characteristics ad study the impact of space vehicle charging potentials in the vicinity of the space shuttle through the acquisition of on-orbit data in conjunction with the Tethered Satellite System/SPREE experiment.* Quite a bit of work went into the preparation of SPREE hardware for this re-flight mission (TSS-1R), on which the above objective was to be realized. TSS-1 hardware was refurbished and in some instances upgraded. The primary sensors were re-calibrated and new GSE software was written. A detailed discussion of the activities which took place prior to launch and a preliminary analysis of the returned data is presented in section 3.4.

After about a year of 'low level activity' due in part to programmatic uncertainties on the launch vehicle end, DIDM activities were ramped-up in the second quarter of 1995 to meet a new scheduled delivery date of 30-Oct-96. Some functional details of the instrument are provided in section 3.2 and 3.3. An issue which has developed into a real problem for the program is the matter of having the wedge & strip anode made with the thin Gold layer previously discussed. This endeavor turns out to be not as straight forward or trivial an undertaking as it would first appear. Setbacks of various kinds were encountered at just about each step along the way and only a very limited number of successes has been realized to date.

3.2 DIDM Activities

A principal milestone in the DIDM program was achieved around the middle of the report period when the DIDM design review meeting occurred. The proceedings were held at Hanscom AFB and occupied the better part of a day. Approximately twenty five participants were in attendance,

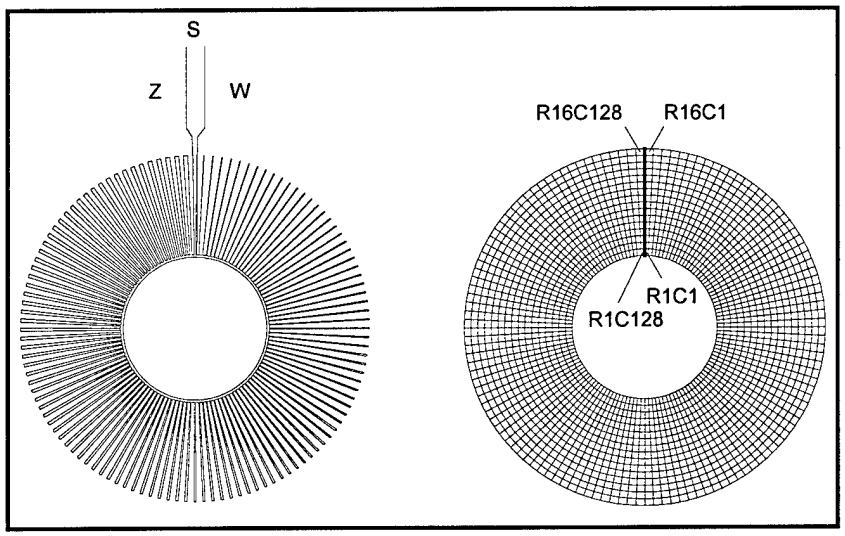

FIGURE 21:
ANODE DETAIL SHOWING ACTUAL STRUCTURE (LEFT) AND EQUIV PIXEL ARRAY MAP (RIGHT).

including out-of-town attendees from TRW (the space vehicle contractor and payload integrator), SMC/TE (the USAF STEP Program office), and Aerospace Corp. (USAF Payload support). By all accounts, the material presented was well received. It was disclosed that instrument capability will exceed all of the basic functionality requirements. In most instances, the design will be better than the requirements by a factor of three to four. In one instance, that of the minimum accumulation time for particle counts in the Drift Meter mode of operation, the requirement is that a 125 msec period be accommodated. The design will afford a 25 msec accumulation time, which is better than the requirement by a factor of five. Another dramatic illustration of design capability is in the dynamic range for particle counts. Existing analog instruments can at best, range from a few thousand particles to tens of thousands per second, in count rate. It is expected that DIDM will reliably count from between zero per second to 10^5 per second and thereby extend the achievable count rate range by at least two orders of magnitude. A general overview of the instrument design follows. No discussion of the sensor head is included, as its design and manufacture was largely the responsibility of PL/GPSG.

3.2.1 DIDM Instrument Design Overview

The prime design objectives are: (i) provide a *proof-of-concept* instrument, which has the capability of both a Retarding Potential Analyzer and a Drift Meter, in a small, light (max. 5 lbs), low power (max. 5 W) package. (ii) reliably achieve count rates down to 10^2 per sec in as low as 125 ms

accumulation interval. The intent is to produce an instrument with better dynamic range (> two orders of magnitude), than that presently achievable with existing analog sensors, on operational spacecraft. Two nearly identical Detectors are contained within the DIDM instrument. Functionally, each is made up of two distinct sections-an ion optics and detection head; and power supply & processing electronics.

3.2.2 *Wedge & Strip* Anode Design

Ions are detected on a novel *wedge & strip* anode, which serves as the collector behind a Micro-Channel Plate. The *wedge & strip* is capable of distinguishing incident particles within 2.5° from *zenith* (θ) and 2.8° around zenith or *in azimuth* (ϕ). This is accomplished by mapping θ into 16 radial elements *(r)* and ϕ into 128 circumferential *(c)* elements on the anode. Thus making it possible to distinguish incident particle on any out of a total of 2048 (16 x 128) pixel elements. An anode detail showing the physical structure of the device, and its equivalent pixel array map, are shown in Figure 21. Pixel address determination is done in hardware in the instrument, within what is referred to as the *front-end* or analog electronics.

3.2.3 DIDM Analog Electronics Design

As can be seen in Figure 22, which is a block diagram of DIDM analog electronics, there are three principal sections to the instrument's analog design. These are: (i) the Sensor Preamplifier; (ii) Shaping Amplifier; (iii) Digital Signal Processor. The Preamplifier receives signals from the anode for each wedge, strip and z element. The sensors connect directly to the Preamplifier Board in the instrument, and an integrated output for each anode element is generated. Some six preamplifier modules and corresponding baseline restorers are incorporated in the instrument for the two instrument sensors.

The shaping Amplifier first differentiates the preamplifier signals in order to create a fast rise-time pulse with a long tail which decays to a baseline. The fast edge is then filtered in a second-stage operation, which results in a rounded pulse which an A/D converter can sample. The anode element signals are next combined to produce a reference sum. The wedge pulse and the strip pulse are compared to this sum in a one quadrant analog divider circuit. The ratio produced from the divider is the equivalent *r* or ϕ coordinate for an ion entry to the sensor. Additional circuitry detect the peak of each of the sum signals and generate a start-conversion signal for the appropriate A/D converter. The hardware to implement this functionality utilizes twelve amplifier modules, four divide circuits and two peak detectors.

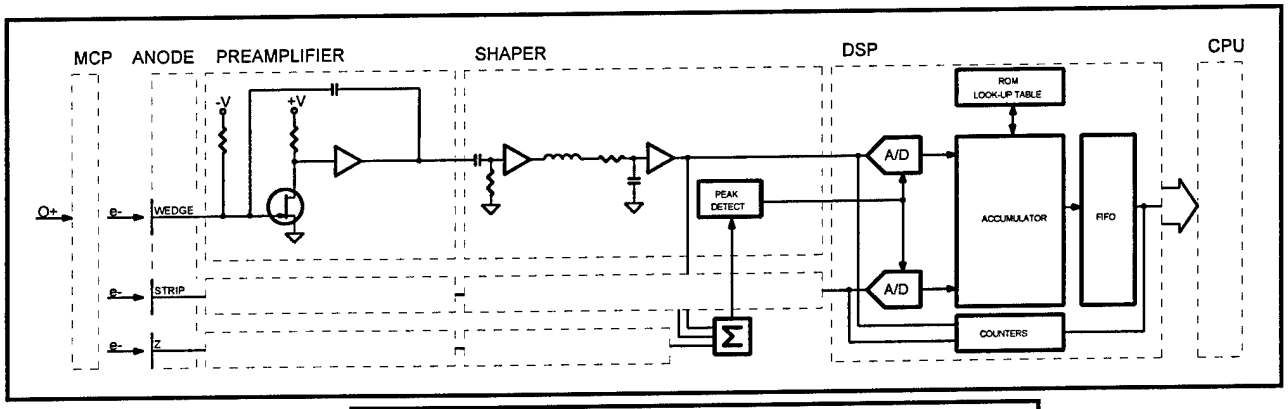

FIGURE 22: DIDM ANALOG ELECTRONICS BLOCK DIAGRAM

The final element in the front-end electronics is the DSP, which digitizes the r and ϕ coordinate values. This functional element acts in similar fashion to a multi-channel analyzer. A Static Random Access Memory module (SRAM) emulates over four thousand 16-bit counters (one for each pixel in the array map of each sensor). A Field Programmable Gate Array (FPGA) increments the SRAM at the address corresponding to the determined r and ϕ coordinate values. Finally, when an acquisition period is complete, the FPGA allows the Central Processing Unit (CPU) in the instrument to read the SRAM by having it emulate a First In First Out (FIFO) memory module. A DSP functionality block diagram is shown in Figure 23.

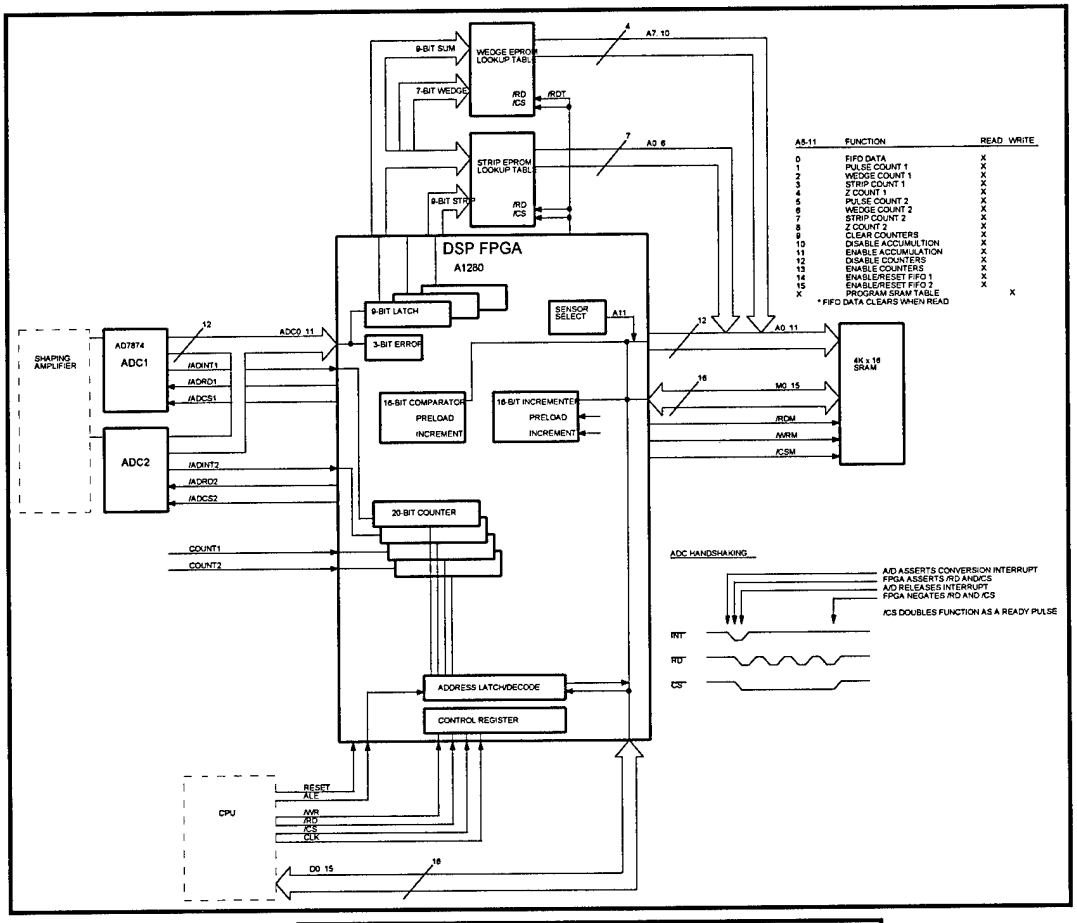

FIGURE 23: DSP FUNCTIONALITY BLOCK DIAGRAM

3.2.4 Other Functional Elements in DIDM

The other key functional elements within the instrument are: (i) power supply; (ii) CPU; and (iii) telemetry interface modules. A brief description of each follows. (i) In addition to providing low voltages (± 5V, ± 12V) to power CMOS and TTL electronic components in the instrument, the MCPs in DIDM requires a -1900V potential difference across them. This is done by generating two different voltages in the power supply module. The first (-2100V) is applied to the front of the MCP. This potential attracts ions which enter the instrument aperture to the MCP, and as such, has a significant influence on the imaging response (i.e. mapping of incident angle to anode output) of the sensors. The second voltage (-100V) is applied to the back of the MCP, and it serves to some extent, to focus the exiting charge cloud into a desirably smaller spot size on the Wedge & Strip anode. The power supply

module also generates the RPA voltages (+33V max.) and entrance gate voltage (+33V), for each sensor. (ii) The instrument utilizes an Intel 80C86 microprocessor at the heart of its CPU, which is the control center of the instrument. All process timing and instrument tasking originates here. (iii) DIDM interface to the spacecraft is based on the MIL-STD-1553B communication protocol. The output from each sensor is sampled and packetized into 64 byte blocks. For the STEP 4 mission, the DIDM data rate is fixed at 640 bytes per second and the data structure is organized in a major-minor frame format, with ten minor frames in a major frame. The major frame data structure is repetitive on a one second basis.

3.2.5 DIDM Operating Modes

There are two basic modes of operation for each sensor. These are: (i) Retarding Potential Analyzer (RPA) mode; (ii) Drift Meter (DM) mode. The particular sensor mode and its corresponding instrument operation will be determined by ground command to the instrument

3.2.5.1 RPA mode: In this configuration, the sum of the counts in all 2048 pixels is reported. A sweep voltage applied to RPA grid, which could be in the range of 0 – 31.733 V. The minimum increment which can be set is 1/30 V. Up to 128 steps are allowed in the sweep profile. The step duration may be set from 25 msec – 6.375 sec. The minimum increment is 25 msec. It is possible to choose between two sample rates in this mode by instrument command. The rates are 20 Hz and 40 Hz. The accumulation interval for either extends from 25 – 500 msec, with a minimum increment of 25 msec. Both the magnitude and duration of a sweep is preset in a table, with up to 16 tables allowed. Additionally, it will be possible to offset the table values by an amount which is commanded from the ground.

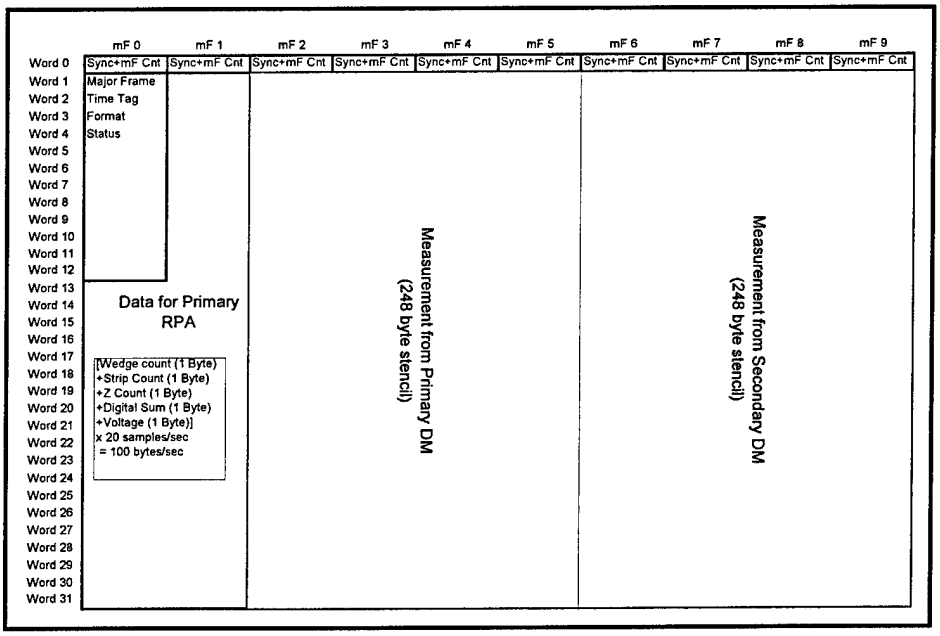

FIGURE 24: DRIFT METER MODE TELEMETRY STRUCTURE (1 OF 6)

3.2.5.2 Drift Meter Mode: The on-board micro-processor in DIDM will determine the pixel with peak number of counts in this mode. It will then put this pixel in the telemetry stream and a surrounding subset of pixels. The chosen subset will be pre-defined in a *stencil,* and is selected by ground command. The number and shape of these stencils are currently to be determined, but the information will be provided by PL/GPSG. Three sample rates (2 Hz, 4 Hz & 8 Hz) are possible in

this mode. The accumulation interval is variable from 0 to 0.5 sec, with a minimum increment of 25 msec. It is possible to apply a sweep voltage to the RPA grid in this mode if so desired. The most often used configuration however, will be with the RPA grid grounded. A special case configuration is with the maximum sweep voltage (31.733 V) applied to the grid and the entire pixel map telemetered at the end of the maximum accumulation. period (0.5 sec). This *CAL mode* is to be used to identify *bad* pixels, which must be excluded from peak search. A bad pixel table will be maintained for this purpose.

Another special case configuration is the *Test Pulse* mode in which the electronics which receives signals from the Wedge & Strip Anode are stimulated in a fashion which produces a particular image pattern the instrument output. This feature is particularly useful for testing the instrument and its telemetry interface, in circumstances which do not permit the high voltage to the MCP's to be enabled. It will also be an important on-orbit verification check of electronics functionality.

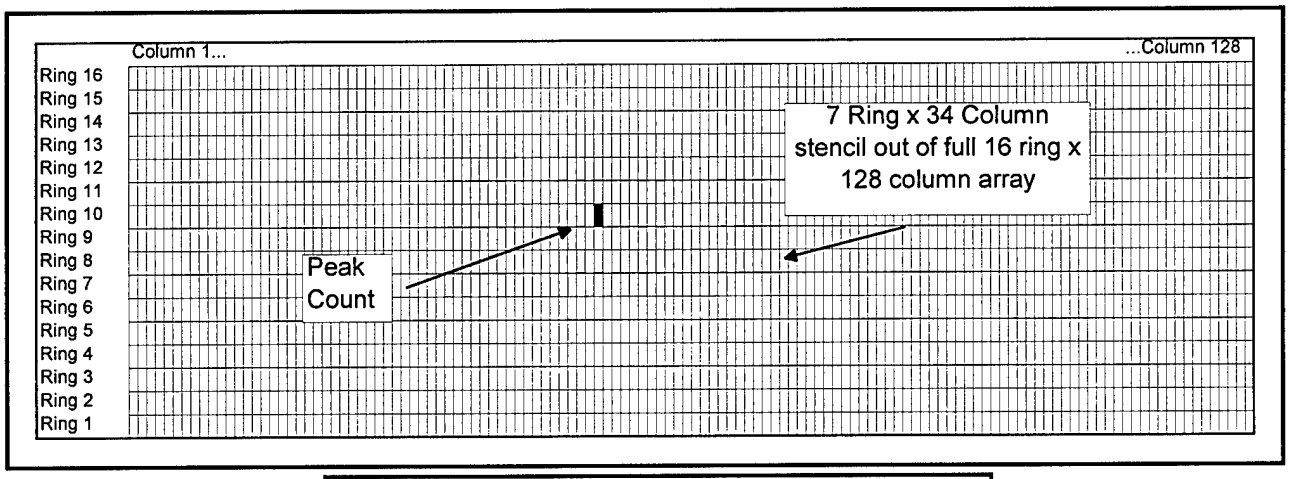

FIGURE 25: ILLUSTRATION OF A POSSIBLE DIDM STENCIL. SHADED PIXELS ARE SAMPLED.

3.2.5.3 Telemetry: The output from each sensor is sampled and packetized into 64 byte blocks, and then transferred via MIL-STD-1553B protocol to the spacecraft interface. The DIDM data rate is 5 kbps ≡ 640 bytes per sec, and the data structure repeats on a one second basis. No science data will be collected from DIDM during period that the spacecraft is in contact with ground (max. 10 min interval for this orbit). However, up to two words per sec of instrument state of health data will be accepted on the 1553B interface, during this time. This allows instrument status to be downlinked and viewed during real time contacts, along with other spacecraft state of health information. There are four analog monitor signals from the instrument which are read directly by Experiment Interface Processor module on spacecraft.

Telemetry will be acquired and formatted in one of two different ways depending on the selected operating mode of the instrument. The possibilities are: Retarding Potential Analyzer (RPA) mode and Drift Meter (DM) mode. In Drift Meter mode, the anode array address and content of the pixel containing the highest number of counts, for the set accumulation interval, is telemetered along with those for a predetermined selection of surrounding pixels. The predetermined selection of surrounding pixels are defined in what is referred to as a stencil. A selection can be made from up to 256 different stencils. An example of a DM mode telemetry packet structure is shown in Figure 24.

The instrument returns data in six different formats in this mode, with each DM configuration having a different telemetry packet structure. Figure 25 illustrates the structure of a stencil.

Only the sum total of all the counts in the anode pixel array is returned in telemetry when the instrument is placed in RPA mode. RPA data is then taken from both sensors and no drift meter data is acquired. DIDM has sufficient memory to accommodate up to 16 RPA sweep tables, with up to 128 steps in each sweep. The period of each step in the table can range from 25 ms to 6.375 ms, and the minimum increment is 25 ms. Step voltage can be step voltage can be selected in the range 0 V to 31.73 V with 1/30 V resolution. A design requirement is that the sweep voltage fed to RPA B be attenuated by 20% from the sensor designated as RPA A.

3.3 DIDM Prototype

3.3.1 Introduction

The DIDM prototype was designed and built for use in characterizing the imaging capability of the instrument's sensors . Its primary purpose is to map the arrival angle of an incident particle, as detected by the *wedge & strip* anode, onto a rectilinear grid with *16 rows (r0...r7)* and *128 columns (c0...c127)* so that two incident angles (θ – polar angle from zenith; ϕ – azimuth angle) could be determined. This grid display is usually referred to as the pixel map. Note that θ maps to r and ϕ maps to c. The opening angle of the sensor is 95°, so the best resolution which can be achieved for θ is $\frac{95°}{2 \text{ x } 16 \text{ rows}} \approx 3°$ per row. For ϕ the corresponding number is $\frac{360°}{128 \text{ columns}} \approx 2.8°$ per column.

The following material provides some indication of the hardware installed in the prototype box, its functionality, and details the display features of the DIDM prototype software as well.

3.3.2 How the Prototype Works

Each incident ion onto the MCP generates an electron cloud, which strikes the *wedge & strip* anode at a location dependent on the incident angle of the ion at the sensor aperture. This anode location is indicated by the respective amplitude of the signals from the wedge, strip and z (area between wedge and strip) elements on the anode. To make the translation, each anode signal is detected by a charge sensitive pre-amplifier, which produces a shaped, low amplitude and very fast pulse (200 ns peak time) at its output. This signal is then fed into a pulse shaper which conditions the signal so that it might be sampled by an analog to digital (A/D) converter. A calculation is then made in software for polar angle (θ), based on the amplitude of the wedge signal to the sum of the three signals, and for the azimuth angle (ϕ) based on the amplitude of the strip signal to the sum.

The prototype system does not have a fixed accumulation period for incident events. This interval varies. The A/D converter is enabled 5000 times with a duration window which can last from 41 µs to 100 µs. Of this period, 40 µs is required for the A/D to convert a valid event, so that in actuality, the corresponding accumulation periods are 1 µs to 60 µs. Note that events occurring between 61 µs and 100 µs are not recognized by the system. There is no means of getting at the exact event period in the existing design. That task would be particularly complex since function calls to system time in the PC has a resolution of only 58.8 ms.

The default **Sample Limit** can be changed to 1000 (A/D converter is enabled 1000 times with a maximum duration of 100 µs each time) in the CONTROL display tab. It is for use on PCs which cannot run fast enough to update the graphic objects at a 1 Hz rate after performing the data accumulation tasks. At the 1000 **Sample Limit** setting, the available display period is increased from 0.5 s to 0.9 seconds.

3.3.3 Running the Software

The DIDM prototype executable is a WINDOWS 3.1® or WINDOWS 95® application, which means that it will only run in one of these WINDOWS environments. To start the program, it is necessary simply to click on the DIDM icon (the Amptek logo) in the MAIN menu selections of the WINDOWS desktop, and the default GSE screen shown in Figure 1 will then appear. If the sensor is not in an ion beam, the data fields will of course, be empty.

3.3.4 GSE Displays

3.3.4.1: Top Level Buttons:

Figure 26 shows the default GSE display, it appears when the program starts-up and can also be obtained by clicking on the **Map** display tab near the top of the screen. There are five control buttons in a row at the very top of the display. They are: (i) **Run;** (ii) **Stop;** (iii) **Save;** (iv) **Next** and (v) **Clear.** The functionality of each is as follows:

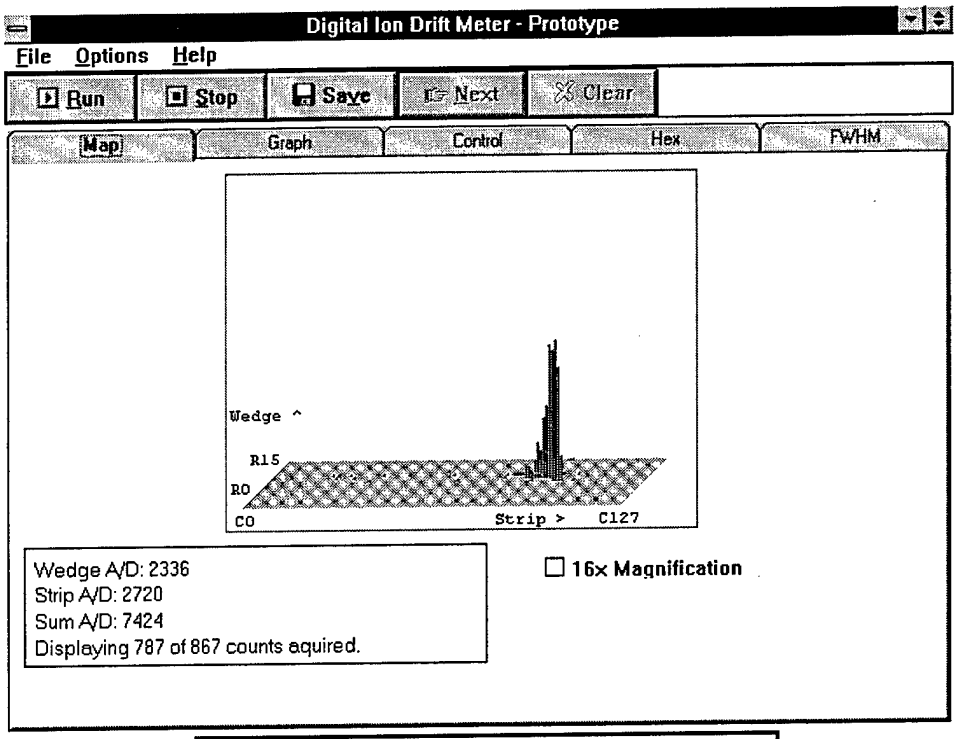

FIGURE 26: DEFAULT GSE SCREEN — TOP LEVEL BUTTONS & MAP DISPLAY

3.3.4.1.1 Run

Selecting this button re-enables the sensor electronics to resume processing inputs, after it is stopped.

3.3.4.1.2 Stop

Selecting this button prevents the sensor electronics from processing inputs. The display screens will remain frozen with data from the last accumulation period.

3.3.4.1.3 Save

Selecting this button transfers the counts in the pixel map to a file. The data file name can be specified in the **File** menu, which is part of the standard WINDOWS selections, that appears at the top of the display screen.

3.3.4.1.4 Next

Not currently enabled.

3.3.4.1.5 Clear

Not currently enabled.

3.3.4.2 The Map Display

The pixel map of incident particles onto the *wedge & strip* anode is seen in Figure 26. Some information about system performance is also shown. There are three display areas: (i) the pixel map box in the center; (ii) the diagnostic group box at lower left; and (iii) a **16 x Magnification** check box. Details follow.

3.3.4.2.1 PIXEL MAP

The entire **Map** display reflects status when the screen is refreshed every second. The pixel map is the display in the center of the screen and it shows the distribution of valid incident events in pixel location and number (which is indicated by amplitude). The long axis of the map is azimuth angle location. It is labeled as **C0 Strip > C127** which says that this coordinate is determined from the strip signal and that it increases from left to right in 128 discrete steps. Correspondingly, the short axis is polar angle location. It is labeled **R0 R15 Wedge ^** which indicates that this coordinate is determined from the wedge signal and that it increases from the lower left in 16 discrete steps. For polar angle, the relationship of step to angle is $\frac{95°/2}{16 \text{ steps}} \approx 3°$ per step. For azimuth, it is $\frac{360°}{128 \text{ steps}} \approx 2.8°$ per step. With these two numbers, two components of the incident angle may be determined in cylindrical coordinates.

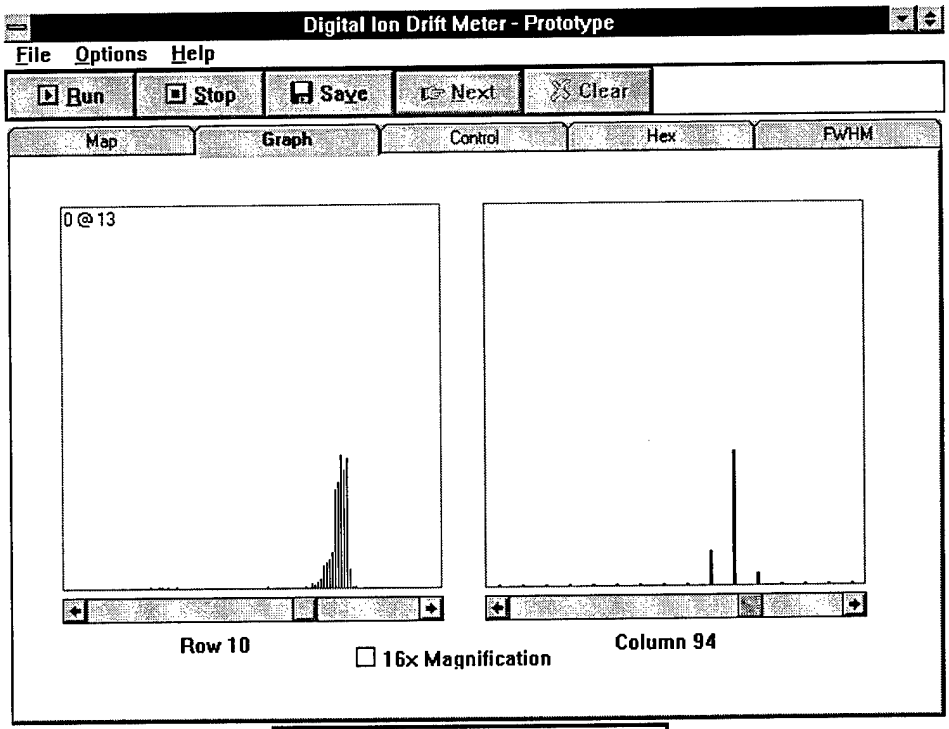

FIGURE 27: THE GRAPH DISPLAY

3.3.4.2.2 DIAGNOSTICS

The diagnostics group box is shown in the lower left of the display, below the pixel map. Four parameters are shown. They are: (i) **Wedge A/D**; (ii) **Strip A/D**; (iii) **Sum A/D**; (iv) **Displaying xxxx of #### counts acquired.**

The wedge, strip, and sum (of wedge, strip, and z) signals are digitized with a 15 bit converter. As a practical matter, only 60% of the maximum 32 k range can be utilized and therefore the highest value which will appear next to **Wedge A/D, Strip A/D**, and **Sum A/D** values is limited to around 25,000.

The **####** number in **Displaying xxxx of #### counts acquired** indicates how many events were detected in 5000 A/D sample periods. Numbers less than 5000 indicate that for 5000 ' ####' sample periods, no event occurred during the 60 μs interval when the A/D was active.

Not all of the counted events are considered to be valid ones. The **'xxxx'** number indicates what are thought to be valid events, and are therefore included among those which make up the pixel map. There are several conditions which disqualify an event from being considered valid. These are: (i) an event which results in **Wedge A/D**, **Strip A/D**, or **Sum A/D** numbers are greater than 20,000. (ii) a negative number in any of the **Wedge A/D, Strip A/D** or **Sum A/D** fields. (iii) a number in either of the **Wedge A/D** or **Strip A/D** fields that is larger than the **Sum A/D** value. Noise conditions are the single most likely source for any of these eventualities.

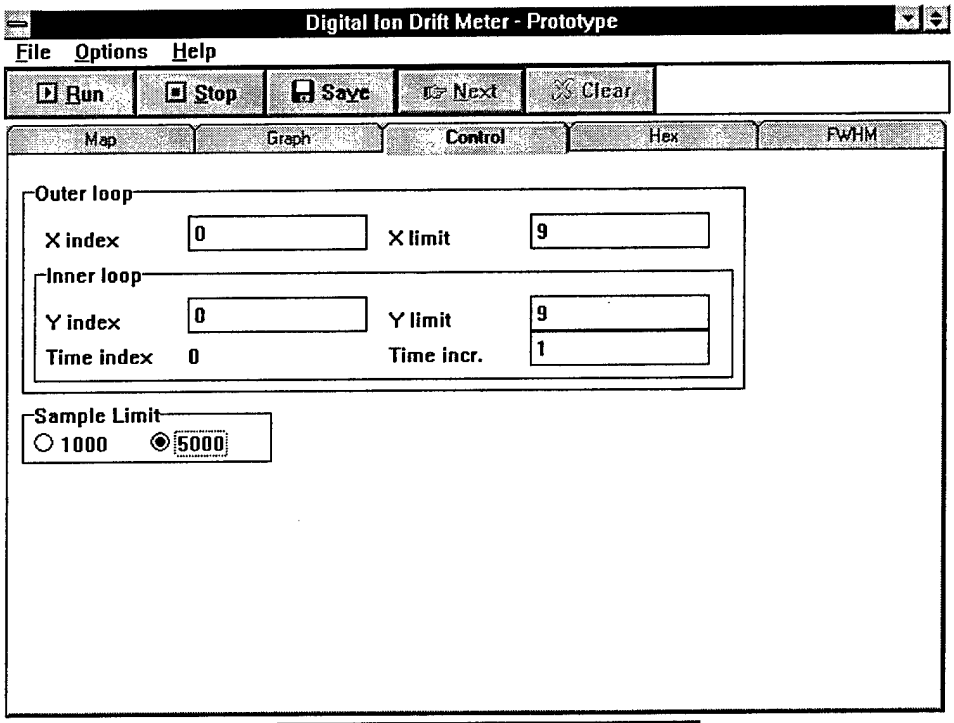

FIGURE 28: THE CONTROL DISPLAY

3.3.4.2.3 16X MAGNIFICATION

This is a single button to the right of the diagnostic block which amplifies all values in the pixel map by a factor of 16 when it is selected. The default amplitude range is about 125 events. In instances when the counts are few in number, the 16x magnification could make the pixel map display more visible.

3.3.4.3 The Graph Display

When the **Graph** display tab near the top of the screen is selected, the display shown above in Figure 27 appears. It shows two 2-dimensional cross sections of the **Map** display. The plot on the left is the view along the row or polar angle axis of the pixel map in Figure 1. That on the right is the view along the column or azimuth angle axis. Both plots have a scroll bar which makes it possible to scroll through the full parameter range. It is therefore possible, for example, to search for the row and column with the highest number of counts, from among the 16 possible choices for rows or the 128 choices for columns.

A 16x Magnification button is also available at the bottom of the screen, for viewing enhancement of this display.

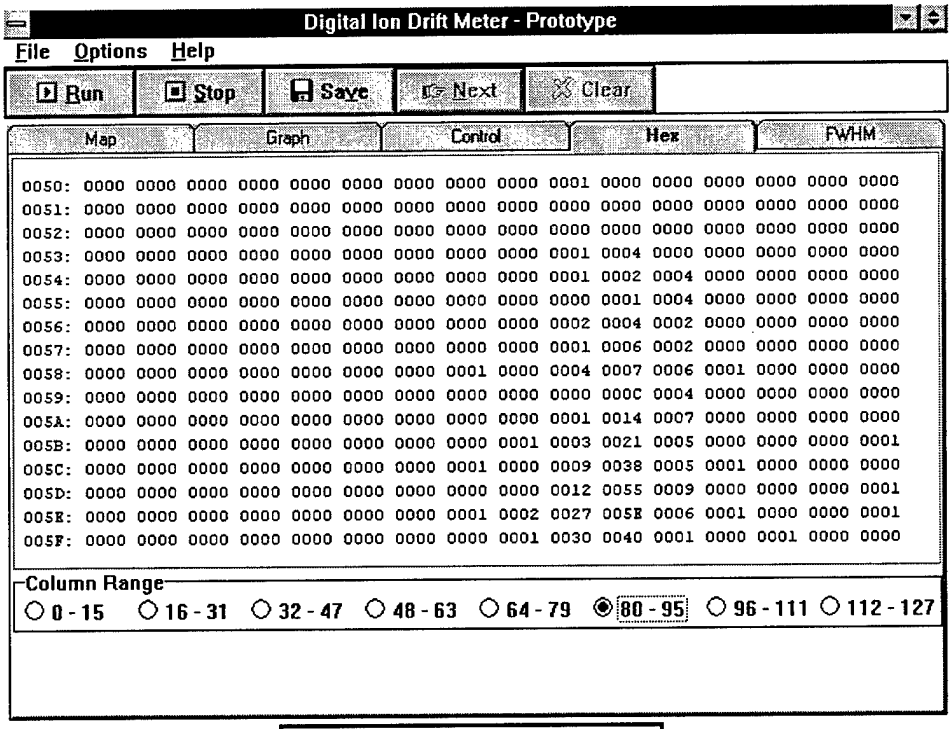

FIGURE 29: THE HEX DISPLAY

3.3.4.4 The Control Display:

When the **Control** display tab near the top of the screen is selected, the display shown above in Figure 28 appears. The **Sample Limit** display at the bottom left of the screen is the only functional aspect of this window at present. The default value is 5000, which is the number of times the A/D converter is enabled (for a maximum duration of 100 μs) to acquire an event. When changed to 1000, the A/D converter is enabled only 1000 times. This latter setting is intended for use on PCs which cannot run fast enough to update the graphic objects at a 1 Hz rate after performing the data acquisition tasks. At the 1000 **Sample Limit** setting, the available display period is increased from 0.5 s to 0.9 seconds.

3.3.4.5 The Hex Display

When the **Hex** display tab near the top of the screen is selected, the display shown above in Figure 29 appears. It is a 16 x 128 array, containing the number of *hits* in each pixel of the **Map** display. Note that the columns in this display corresponds to the wedge or polar angle axis of the **Map** display, while the rows corresponds to the strip or azimuth angle axis. Only 16 of these are displayed at a time. The full range is covered by the 8 buttons which appear in the **Column Range** block at the bottom of the display. All of the numbers in the display, including the column number in the leftmost column, are in hexadecimal format.

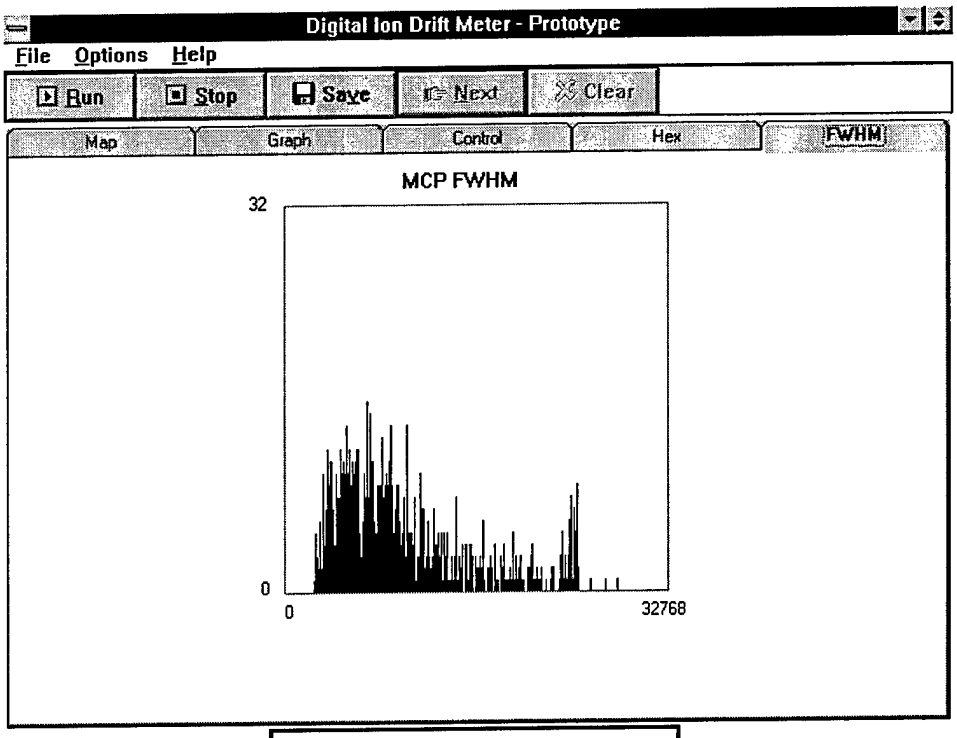

FIGURE 30: THE FWHM DISPLAY

3.3.4.6 The FWHM Display

When the **FWHM** display tab near the top of the screen is selected, the display shown above in Figure 30 (or something like it) appears. This is a diagnostic display of the MCP output. The full MCP output onto the anode is measured by the Sum (Σ) signal, which is the addition of the signals from the three anode elements (wedge + strip + z [the area between the wedge and strip]). Both the polar (θ) and azimuth (ϕ) angle calculations require the Σ signal, which is effectively digitized by a 15 bit (0 – 32k range) analog to digital converter.

Only 60% (representing 6 volts) of the full range can be realized in the prototype and this is seen on the x-axis of the display, which represents MCP output amplitude in the range 0 to 32k. The y-axis represents frequency of occurrence for each amplitude. The spectra shown is thus a histogram showing the frequency of specific outputs. It is a useful indicator of MCP gain, for this shape changes over time with MCP use, and with the magnitude of MCP bias.

The shape of the ideal distribution would be close to the characteristic distribution curve provided with the specific MCP. It should not have the spike which appears on the tail of the curve shown in Figure 5. This is an artifact of the prototype hardware. It indicates that the pulse shaping response saturates, and becomes non-linear around 20k.

3.3.5 Hardware

The three principal sections of the analog electronics for the DIDM flight instrument were incorporated into the custom prototype hardware design. In addition, hardware and software were added to allow a RS-232 interface with a desktop computer which served as the GSE for the unit. Direct input from one sensor was afforded through short BNC connections and an analog output signal (a total count indicator) was provided to aid in the sensor characterization studies. A block diagram of the constituent elements is indicated below in Figure 31.

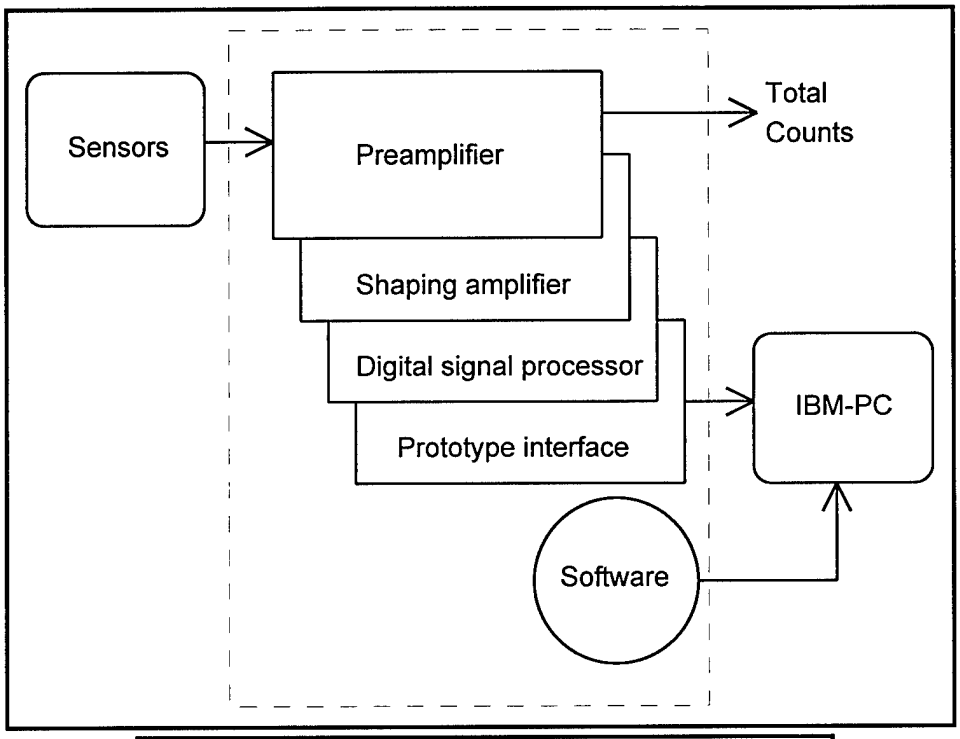

FIGURE 31: BLOCK DIAGRAM OF DIDM PROTOTYPE SYSTEM

3.4 SPREE Activities

Hardware for the Shuttle Potential and Return Electron Experiment (SPREE) was designed and built by Amptek, Inc. under a separate contract, as a key experiment for the Space Shuttle's Tethered Satellite System 1 (TSS-1) mission, which flew in August 1992. Amptek, Inc. performed a number of tasks in support of the SPREE re-flight (TSS-1R) mission, which occurred in February 1996. The work fell largely into three distinct areas. They are: (i) Instrument Refurbishment; (ii) Launch vehicle experiment Integration & Test support; (iii) Pre-launch flight simulation and On-Orbit mission operations support.

A brief discussion on each of these tasks follows: (i) Some refurbishment of SPREE hardware was necessary to accommdate the TSS-1R mission. This was not an extensive undertaking, but rather more of a selective effort, which was carried out to fix known deficiencies. The specific repairs were: (a) Wave-particle correlator (SPACE) upgrade; (b) Rotary table correction to ensure synchronization; (c) Adjustment of the electrostatic analyzer (ESA) thresholds; (d) Re-calibration of the ESAs; (e) FDR inspection and repairs following thermal vacuum test mishap. (ii) Launch vehicle experiment Integration & Test support was of the form usually extended to install, checkout and verify proper functionality of space experiments before launch. This activity occurred at the launch facility at Kennedy Space Center, FL. (iii) Pre-launch flight simulation and On-Orbit mission operations was supported by six Amptek, Inc. personnel, who were integral to the experiment team at mission operations control, at the Marshall Space Flight Center, in Huntsville, Alabama.

All results to date show that the SPREE hardware functioned without any anomalies. Quick look analysis indicates that the change to the SPACE modes worked appropriately. The rotary table synchronization problem which occurred on the TSS-1 mission was completely fixed. The adjustment to the ESA thresholds also appears to have been adequate; on-orbit, a successful modification was made to the Orbiter charging algorithm to accommodate this.

TSS-1R was a fairly unique mission in that it was the largest high-power spacecraft ever flown. The data set collected presents an unprecedented opportunity to scientifically analyze the interactions between spacecraft and the ionosphere. The following material is a brief summary of some of the preliminary findings from the SPREE measurements of wave-particle interactions during the mission. The material was compiled by Dr. M. Paul Gough of the University of Sussex in Great Britain, a noted particle-correlator expert, whose services were solicited to provide both operational and data analysis software for the mission.

3.4.1 The SPREE Instrument

The SPREE sensors consist of two rotating electron spectrometers constructed as triquadraspherical electrostatic analyzers (Oberhardt *et al*, 1994). The geometric factor of sensor A is two orders of magnitude higher than that of sensor B. Each sensor has an entrance aperture 100° x 8° fan that combined with the sensor rotation gives a full 2π steradians view out of the orbiter bay. The measured energy range is 10eV to 10keV in 32 logarithmic steps. The particle correlators consist of both high frequency units and low frequency units. The six high frequency electron Auto-Correlators, (ACF), cover the ranges of 0-10MHz, 0-2.5MHz and 0-0.625MHz on TSS-1. These were modified to 0-10MHz, 0-5MHz on TSS-1R. There were six low frequency electron and six low frequency ion ACF covering the ranges 0-10kHz, 0-5kHz, and 0-1.25kHz. Artificial Neural Network, ANN, were used for real-time analysis. Post flight the ACF were Fast Fourier Transformed, FFT, on the ground. These correlator results were obtained during DC operations of the FPEG electron gun (Agüero *et al.*, 1994). Spectral data was reported previously by Hardy et al. 1995.

3.4.2 MegaHertz Electron Modulations

Very strong MHz electron modulations are seen across a wide energy range whenever the 1keV FPEG beam is close to 90° pitch angle, Gough *et al.*, 1995. Figure 32 shows a typical example. The FPEG beam pitch angle was set by the attitude of orbiter relative to terrestrial magnetic field. The measured energy range of modulations extends up to the 1keV FPEG beam energy for electrons measured at 90° pitch angle, but is limited to only a few tens of eV in 0° pitch angle returning electrons, Figure 33.

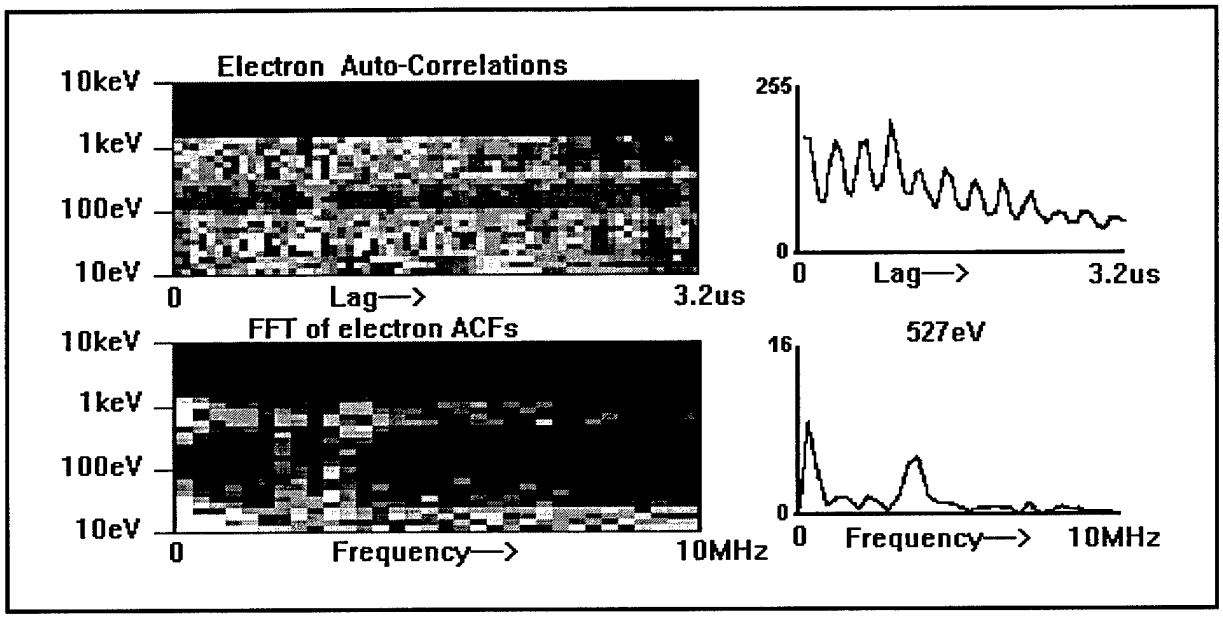

FIGURE 32: AN EXAMPLE MEASUREMENT CLOSE TO 90° PITCH ANGLE. ELECTRON ACF AND FFT ARE SHOWN PLOTTED AGAINST ELECTRON ENERGY ON LEFT WITH AN INDIVIDUAL SINGLE ENERGY ACF / FFT TO RIGHT.

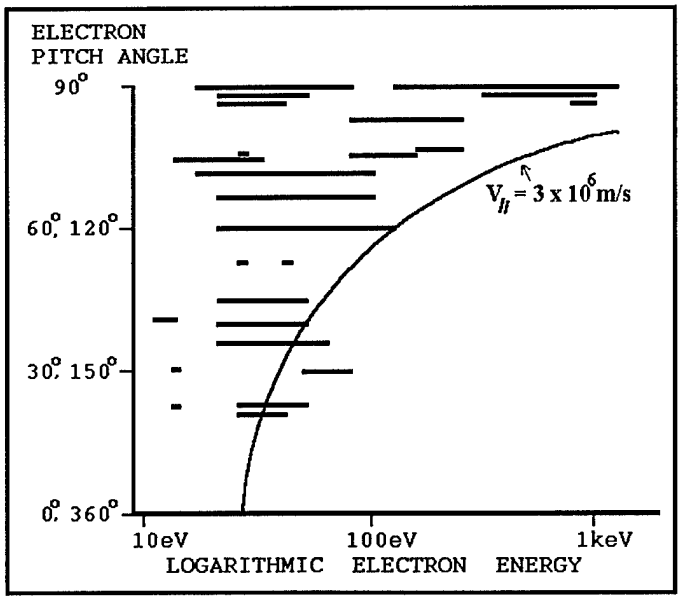

FIGURE 33: OCCURRENCE OF MHZ ELECTRON MODULATIONS IS LIMITED TO LOW V_{PAR} FOR BEAM PITCH ANGLE = 90°.

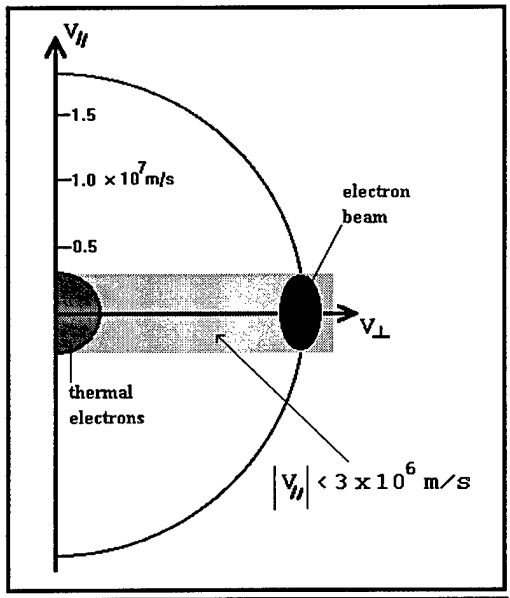

FIGURE 34: EXPLANATION OF MHZ WAVE PARTICLE INTERACTIONS WHEN FPEG PITCH ANGLE = 90°

The MHz electron modulation mechanism is explained as a velocity resonant WPI at parallel resonant velocity, V_{par} , given by,

$$V_{par} = (\omega - n \omega_{ce}) / k_{par}$$

where, ω is the angular wave frequency, ω_{ce} is the electron gyrofrequency, n is an integer (Landau n=0, cyclotron n=1..), and k_{par} is the parallel wave number. At 90° pitch angle the FPEG electron beam has the same narrow range of low V_{par} ($<3 \times 10^6$ ms^{-1}) as thermal electrons and are thus in resonance with the same waves, Figure 34.

Upper hybrid waves generated on the df(v)/dv<0 edge of the FPEG electron beam damp directly on the thermal electron population. Note both wave source and wave sink energy bands are evident in modulations in Figure 32. These results compare well with previous particle correlator measurements of modulated natural electrons above aurora, Gough and Urban, 1983 & Gough *et al.*, 1990. Artificial DC electron beams provide the source of free wave energy in a similar way to natural auroral electron beams.

3.4.3 KiloHertz Electron Modulations

DC FPEG electron gun firings are observed to produce KHz electron modulations much more often than MHz modulations, as they appear over a wide range of FPEG beam pitch angles. A typical example is shown in Figure 35. where the raw ACF are plotted against electron energy. Also shown are the energy-frequency matrices generated (i) post-flight by the use of FFT, and (ii) in real time by the on-board 'expert'. These kHz phenomena were in fact 'discovered' by the on-board 'expert data analyst' (Artificial Neural Network, ANN).

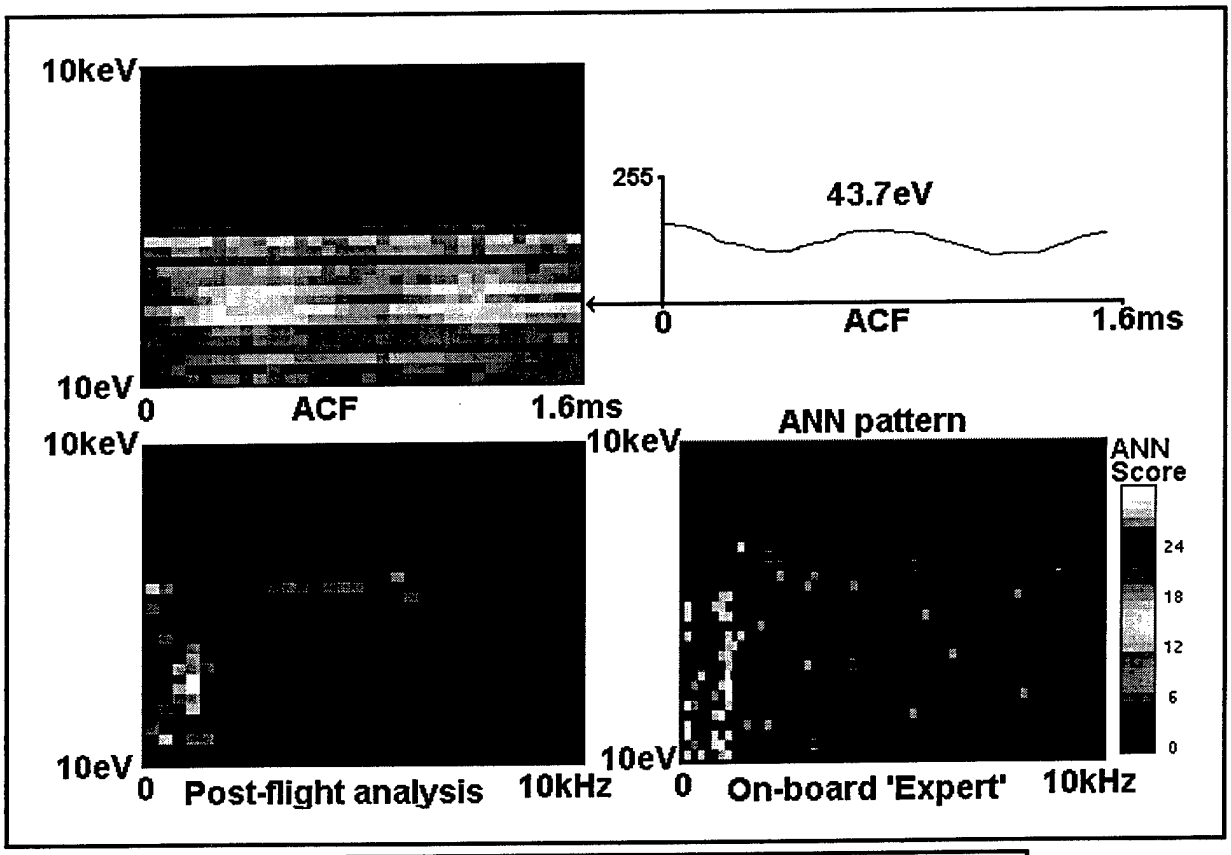

FIGURE 35: KHZ ELECTRON MODULATIONS IN RAW ACF, REAL-TIME ANN, AND POST-FLIGHT FFT.

Although the kHz modulations can be produced over a wide range of FPEG pitch angles the observed modulated electrons are usually confined in electron energy and electron pitch angle corresponding to low $V_{par} < 3x\ 10^6\ ms^{-1}$as for the MHz modulations. At the geomagnetic equator the confinement is to very low $V_{par} < 1.4 \times 10^6\ ms^{-1}$. Returning electron beams are often observed with much reduced V_{par} but with V_{perp} close to the emitted beam, Figure 36. Those at zero V_{par} are thought to correspond to electrons that have undergone strong velocity resonant WPI (probably at MHz that can not be seen due to phase smearing) removing the V_{par} component, while the others have also experienced collisions with neutrals.

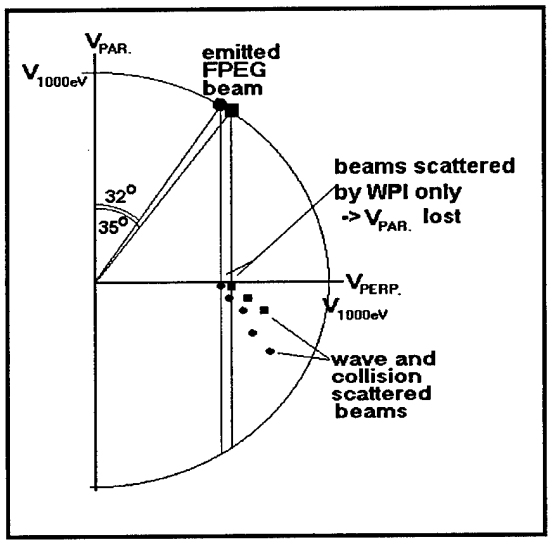

FIGURE 36: LOCATIONS IN VELOCITY SPACE OF RETURNING ELECTRON BEAMS RELATIVE TO EMITTED FPEG BEAMS.

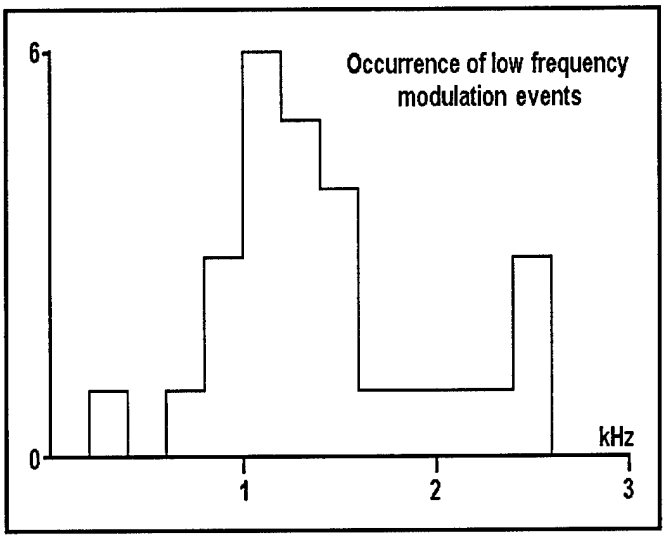

FIGURE 37: KHZ MODULATION FREQUENCIES OF 25 EVENTS

Observed modulation frequencies are spread over the range 300Hz to 2.5kHz but with two preferred frequencies ≈ 1.25kHz and 2.5kHz, Figure 37. The highest modulation frequencies are only observed when the FPEG beam is pointing away from the atmosphere. A total of 25 events are summarized in the following table:

Direction of beam	< 2kHz	>2kHz
Away from atmosphere	8	5
Towards atmosphere	12	0

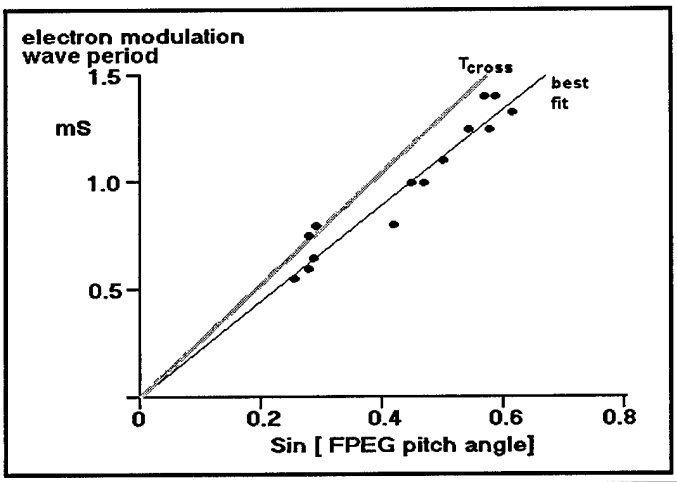

FIGURE 38: DEPENDENCE OF MODULATION PERIOD ON FPEG PITCH ANGLE AT THE GEOMAGNETIC EQUATOR.

On one occasion at the geomagnetic equator when the orbiter attitude varied rapidly the change in FPEG pitch angle was accompanied by a change in electron modulation frequency. The observed modulation period was close to the time, T_{cross} taken by the orbiter to cross the electron beam, as seen in Figure 38. Throughout this time most of the electron distribution was strongly peaked at 90°, indicating that WPI were predominating over collision effects.

3.4.4 Summary

To summarize the kHz observations, electron modulations are observed from a few hundred Hz to almost 3kHz during DC FPEG electron beam firings over a wide range of beam pitch angles. Observed wave frequencies do not fit an expected wave dispersion branch, being above the ion cyclotron but below the lower hybrid frequency. In one event at the geomagnetic equator during orbiter attitude changes the FPEG beam pitch angle varied rapidly with a corresponding modulation frequency variation over a 3:1 range. This frequency change was such as to maintain the observed modulation period equal to the time for the orbiter to cross the electron beam. Electron modulations are seen in electrons with $V_{par} < 3 \times 10^6 ms^{-1}$ but modulations at the geomagnetic equator are even more confined to $V_{par} < 1.4 \times 10^6 ms^{-1}$. Higher frequencies >2kHz are only observed when the effects of atmospheric collisions are least with the beam pointing away from the atmosphere. Weak returning electron beams are often seen with lowered V_{par}. corresponding to combined effects of WPI and collisions. Previous studies by Feng *et al.*,1992 showed oblique electrostatic waves were generated by the Spacelab2 electron beam and noted strong interference patterns in the plasma wave data. The source of these waves was found to be the electron beam.

An explanation of the kHz electron modulation mechanism is as follows: WPI and electron-neutral collisions contribute to filling in the emitted electron beam and provide the returning electrons measured by SPREE. High frequency MHz WPI like those observed to occur when FPEG pitch angle ~ 90° (discussed in previous section) probably occur at most FPEG beam pitch angles where the distribution function contains regions of df(v)/dv <0. However we cannot observe MHz modulations on the orbiter at events other than the 90° due to phase smearing over the sum of many long return paths. The kHz waves are explained by the geometry of the disturbance created by the passage of the orbiter, electron beam, and return electron beams through the local ionospheric plasma at 8 km s^{-1} above the ion acoustic speed. Waves are generated with periods equal to the time, T_{cross}, taken for the orbiter to cross the combined primary and return beam disturbance, (T_{cross} = overall beam diameter / orbiter velocity). Much of the time atmospheric collisions increase the effective beam diameter and hence reduce the modulation frequency. This interpretation is supported both by geomagnetic equator observations of varying period with beam pitch angle and also by the occurrence of >2kHz modulations being limited to when the beam is pointing away from the atmosphere. A fuller account of these observations will be given in Gough *et al.*, 1996.

3.4.5 References

Agüero, V., P. M. Banks, B. Gilchrist, I. Linscott, W. J. Raitt, D. Thompson, V. Tolat, A. B. White, S. Williams, and P. R. Williamson; *The Shuttle Electrodynamic Tether System (SETS) on TSS-1,* Il Nuovo Cimento, 17, 49,1994.

Feng, W., D. A. Gurnett, and I. H. Cairns; *Interference patterns in the Spacelab-2 plasma wave data: Oblique electrostatic waves generated by the electron beam,* J. Geophys. Res., 97, 17005, 1992

Gough, M. P., and A. Urban; *Auroral beam plasma interaction observed directly,* Planet. Space Sci., 31,875, 1983.

Gough, M. P., P. J. Christiansen, and K. Wilhelm; *Auroral beam-plasma interactions: Particle correlator investigations,* J.Geophys. Res., 95, 12287, 1990

Gough, M. P., D. A. Hardy, M. R. Oberhardt, W. J. Burke, L. C. Gentile, B. McNeil, K. Bounar, D. C. Thompson, and W. J. Raitt; *Correlator measurements of MegaHertz wave-particle interactions during electron beam operations on STS 46,* J. Geophys. Res., 100, 21561, 1995.

Gough, M. P., D. A. Hardy, W. J. Burke, M. R. Oberhardt, L. C. Gentile, C. Y. Huang, B. McNeil, K. Bounar, D. C. Thompson, and W. J. Raitt; *Heating and low-frequency modulation of electrons observed during electron beam operations on TSS-1,* submitted to J.Geophys. Res., 1996.

Hardy, D. A., M. R. Oberhardt, W. J. Burke, D. C. Thompson, W. J. Raitt and L. C. Gentile, *Observations of electron beam propagation perpendicular to the Earth's magnetic field during TSS-1 mission;* J.Geophys. Res., 100, 21523, 1995.

Oberhardt, M. R., D. A. Hardy, W. E. Slutter, J. O. McGarity, D. J. Sperry, A. W. Everest, A. C. Huber, J. A. Pantazis, and M. P. Gough; *The Shuttle Potential and Return Electron Experiment (SPREE),* Il Nuovo Cimento, 17, 67, 1994.

4.0 TASK #3—OEDIPUS-C EFFORTS

4.1 Summary of Activities

As it was first envisaged, the objectives of Task #3 were to be accomplished as part of the Waves in Space Plasma (WISP) experiment. This was to be a collaborative effort between NASA and the Canadian Space Agency with three primary objectives. These were to: (1) study the physics of electromagnetic and electrostatic wave propagation in ionospheric/magnetospheric plasmas, especially as it relates to wave-particle interactions. (2) study antenna-plasma interactions in space and (3) investigate large scale dynamics and structures in the ionosphere. The diagnostic tools to realize these ends were to be a pair of very wide coverage Electrostatic Analyzers, a pair of Langmuir Probes, E field Probes and an AC Magnetometer.

Work effectively commenced on this effort in the summer of 1991, when Amptek, Inc. personnel attended a kick-off meeting at the GE Government Services facility in Maryland on August 5. Scheduling and testing issues were at the forefront of the discussions then, although the main focus of the meeting was a review of the preliminary Interface Control Document. Over the course of the next twelve months, various gatherings were convened to discuss among other things the following: (1) electrical and mechanical design issues, for the instruments themselves, as well as, for subsystems within them; (2) flight objectives and operations concepts for the SWIPE experiment; (3) tasking of efforts between PL/GPSP and Amptek, Inc.

The scope of the task was closely reviewed in the first half of 1993 and the engineering effort in particular was closely scrutinized in preparation for a Preliminary Design Review, which was due to occur in the second half of the year. Some effort was also put into considering how data would optimally be returned from the instruments in the payload, and analyzed on the ground. A consultant, Dr. M.P. Gough of the University of Sussex, U.K., who is a recognized authority on space plasma interactions and who had collaborated with PL/GPSP on previous pre-cursor endeavors, was retained to assist in the hardware design and analysis software, for this program.

In January 1993, the course of action and instrument implementation techniques Amptek, Inc. had embarked on for SWIPE were directed to a sounding rocket experiment designated OEDIPUS-C (**O**bservation of **E**lectric Field **D**istributions in the **I**onospheric **P**lasma: A **U**nique **S**olution). The objectives of OEDIPUS-C were identical to those of SWIPE and were also part of the NASA-Canadian Space Agency collaborative effort on WISP. The OEDIPUS-C experiment was slated to fly earlier than the shuttle launched WISP payload which was eventually cancelled. A kick-off meeting was held at Hanscom AFB on 4/15/93, to discuss the conceptual design of the principal diagnostic instrument—an Electrostatic Particle Instrument (EPI)—and to do some preliminary planning for the mission. Amptek, Inc. personnel were participants in the proceeding, for while the company was not tasked with providing the EPI, it was responsible for: (i) the particle correlators which processes the instrument's outputs directly, as well as, (ii) the telemetry output which goes to the downlink transmitter. Program milestones were also established. The OEDIPUS-C launch date was identified as Dec. 1, 1994. Hardware completion was targeted for six months prior, and a design review was set for Nov. 30, 1993.

By the first quarter of 1994, much of the task of designing and building the electronics module for the EPI instrument was completed. The necessary pair of flight units , along with a flight spare, were manufactured and extensively tested with test software written for that purpose. Work was by then underway on writing the flight software, a task which was finalized in the succeeding three months. Due to programmatic concerns, the launch date was progressively delayed a total of almost twelve months. This allowed environmental and functional testing to proceed at an unhurried pace.

Additional hardware was designed and built to allow the Ground Support Equipment (GSE) to not only support launch activities, i.e. to receive the downlinked telemetry and display it real-time; but also to facilitate testing of the flight hardware. The GSE electronic module had built-in interfaces to accomplish the following: (i) power the EPI Electronics Module; (ii) simulate the payload interface module on the launcher; (iii) simulate the EPI sensor interface. Therefore, when a flight Electronics Module is connected to a fully enabled GSE Electronics Module, it is possible to stimulate the unit in a known fashion, request data from it in an identical manner to that used during flight, and look at the output telemetry to gauge the unit's performance. This last feature was done on the monitor of a laptop PC, to which the GSE Electronics Module connects.

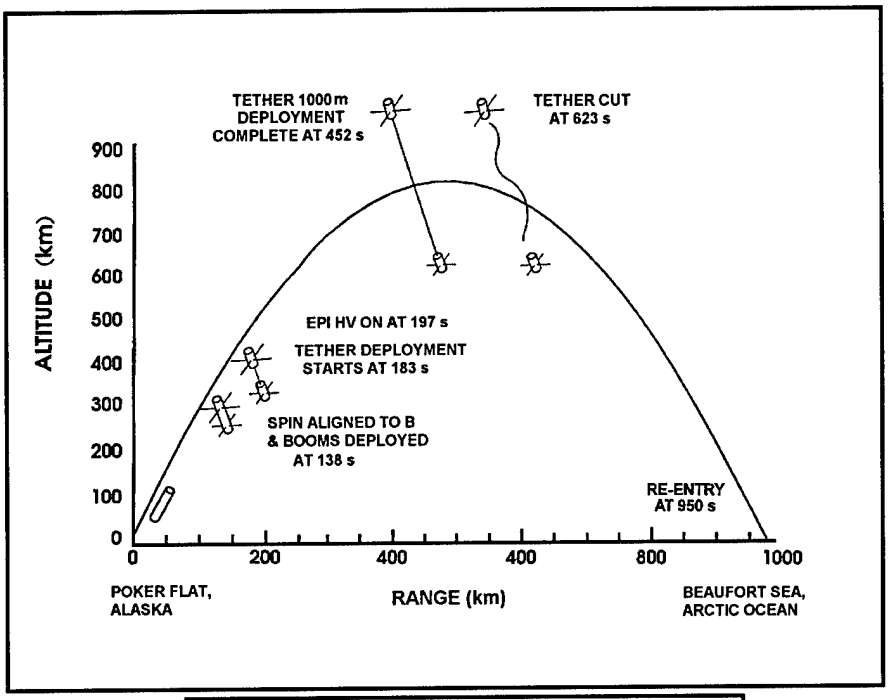

FIGURE 39: OEDIPUS-C LAUNCH MILESTONES

After the Electronics Modules were delivered to PL/GPSG, Amptek, Inc. personnel supported the Integration and Test, Flight Readiness Review and launch phase exercises of the OEDIPUS-C effort. Launch was successful in virtually all respects. The EPIs on both the FORE and AFT sections of the payload worked flawlessly throughout the flight. Flight milestones for the launch are indicated in Figure 19. EPI data was returned starting at 197s into the flight when high voltage to the sensors was enabled. The Electronics Modules provided good data and despite initial difficulties with the quality of the telemetry signal on the data lines, data synchronization was recovered as the units were designed to do, and just about all of the data was acquired on Ground Support Equipment (GSE). Approximately 50 Mbytes of data was saved on the hard disks of each of the two GSE laptop computers, and this was used to make preliminary assessments of wave-particle interactions and to refine the analysis software, until the official range tapes with added ephemeris data were made available for detailed analysis several months later. Initial results from the first in-depth look at the flight data by Dr. Gough follows.

4.2 The OEDIPUS-C Mission

The Canadian OEDIPUS-C auroral sounding rocket was a tethered mother-son payload pair launched 7th November at 06:38UT on a Black Brant 12 from the Poker Flat Rocket Range, Alaska. Both payload sections were well instrumented with space plasma instrumentation from some 11 institutes in Canada, US and the UK. Instruments included on both payloads were a 3-axis magnetometer, a plasma probe, and an energetic particle detector. A HF transmitter, TX, covering the frequency range 0 - 8 MHz, was located on the forward payload, fore, and a HF receiver, RX, was situated on the aft payload, along with instruments to measure the tether current-voltage relationship. The tether was designed to be actively aligned along the Earth's magnetic field. OEDIPUS-C achieved an apogee of 824 km at 517 secs flight time above quiet auroral arcs. Initial tether deployment is illustrated in Figure 39. Deployment continued until the tether was 1200 km in length and was subsequently deliberately cut for comparison measurements. The alignment achieved was stable with negligible coning and held within a few degrees of the field line. Some preliminary results on natural auroral electrons and the TX induced heating of auroral electrons measured by the Energetic Particle Instruments, EPI is presented in the following material.

4.3 The Energetic Particle Instrument (EPI)

The two EPI instruments are triquadri-spherical electrostatic analyzers with a 140° x 8° fan field of view divided into 8 viewing directions of approximately 17.5° x 8° for each channel electron multiplier detector. Each EPI covers the electron energy range 10eV to 20keV in 32 logarithmically separated steps with an energy passband of 10% and geometric factor of 5 x 10^{-2} cm^2 ster. On the fore payload the EPI is downward viewing, while on the aft payload the EPI is upward viewing, with both EPI having one edge of the 140° fan starting viewing from a direction perpendicular to the tether axis.

Each 3.1ms energy step of both EPI units is synchronized to the TX transmitter pulse as shown in Figure 40. As there are 160 TX frequency steps and 32 EPI energy steps it takes several seconds before each frequency-energy combination repeats. TX operations consist of repeated 3s sequences each consisting of six 0.5s TX frequency sweeps with different TX / RX antenna connections and transmitted voltage. Electron detection pulses were processed on-board in the EPI Electronics Modules in three ways. They are:

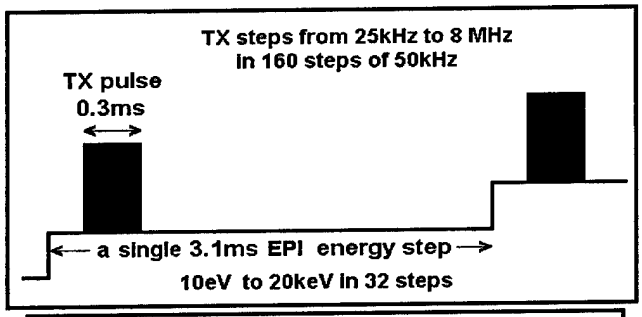

FIGURE 40: SYNCHRONIZATION OF EPI ENERGY STEPS TO TX FREQUENCY STEPS.

(1) Normal count summation over each energy step for electron energy spectra.
(2) Summed time series or superimposed epoch within each energy level as 32 points at 90us resolution.
(3) High frequency electron auto-correlation functions of 32 lags of 62.5ns to cover electron modulations in the frequency range 0-8MHz with 0.125MHz resolution.

This initial report concentrates on the spectral measurements and observed TX heating effects.

4.4 EPI Energy Spectra

Since the EPI energy steps and the TX frequency steps are time period synchronized, electron step count sums can be either plotted against energy to identify spectral features of the auroral electrons, or against TX frequency to emphasize heating resonances.

Whole flight energy spectra from two look directions on each payload are illustrated in Figure 41, which is a nominally color plot, shown here in monochrome, of electron spectra for two view directions on the Fore and Aft payloads. Two quiet auroral arc associated inverted V events can be seen. In general the downward viewing Fore EPI has lower counts than the upward viewing Aft EPI which measures auroral primaries directly.

4.5 Electron Heating at TX Resonances

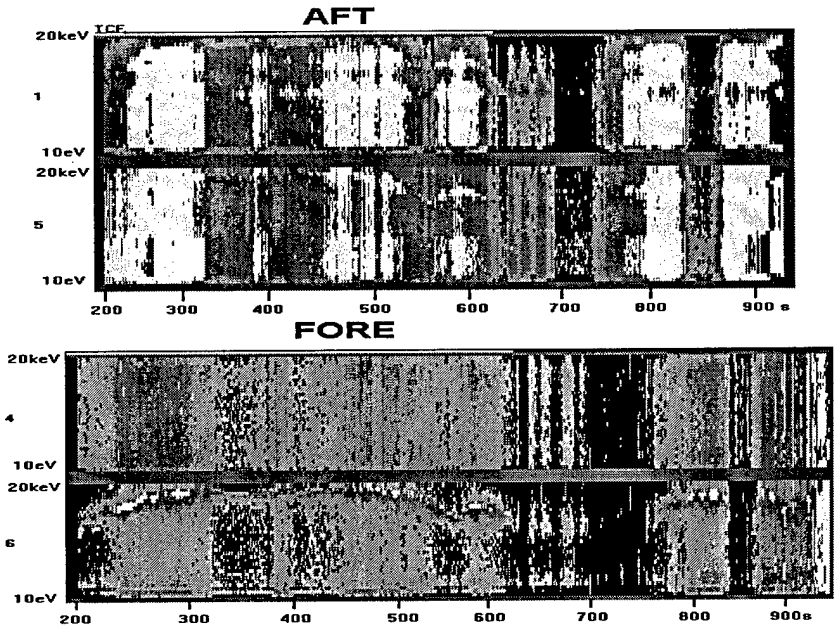

FIGURE 41: ELECTRON SPECTRA FOR TWO VIEW DIRECTIONS ON FORE AND AFT PAYLOADS

Plotting the same EPI data against TX frequency in Figure 43 shows that the auroral electrons are significantly heated around the electron gyro-frequency, f_{ce}, and immediate harmonics for most of the flight. Detailed plots of EPI data just after EPI turn-from 202-233s and near the end of the downleg from 875-930s are shown in Figure 42. Around 210s heating is observed up to at least the fifth harmonic of f_{ce}. Around 900s the main heating occurs in a band that moves upwards from f_{ce} towards $2f_{ce}$. This is identified as the upper hybrid frequency f_{uh}, consistent with the very low cold plasma density measured by other instruments during this flight. For most of the EPI measurement period the plasma frequency is well below f_{ce} so the strong resonance around f_{ce} seen before 900s is also very close to f_{uh}.

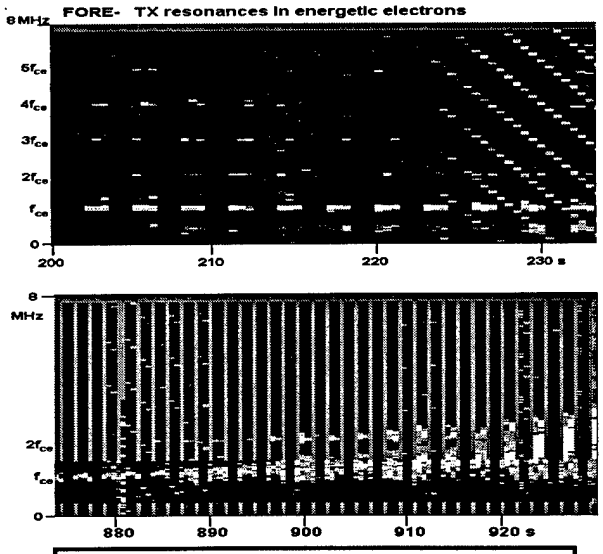

FIGURE 42: DETAILS OF ELECTRON HEATING RESONANCES AT EPI TURN ON AND NEAR END OF FLIGHT.

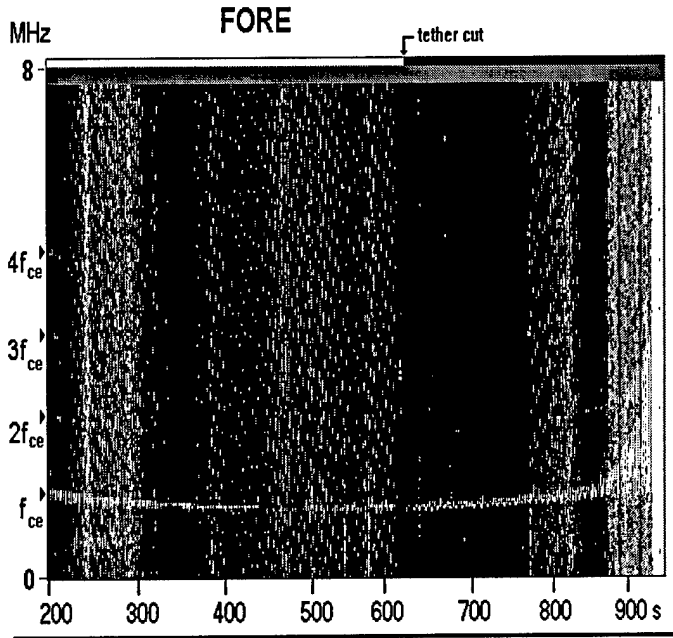

FIGURE 43: WHOLE FLIGHT ELECTRON HEATING AS A FUNCTION OF TX FREQUENCY IN FORE PAYLOAD.

Early in the flight Figures 42 and 43 show a broadband resonance occurring around 0.5 f_{ce} that is either whistler or sheath waves. Note that the chevron patterns in figures 4 & 5 are due to the natural energy spectral features shown in Figure 21 due to the beating of EPI energy stepping against TX frequency stepping. The combined effects of frequency and energy sweeping is detailed in Figure 44 along with an initial interpretation of the TX heating resonances observed in the auroral electrons.

4.6 Electron Response to TX Pulses

Analysis of the more detailed functions, summed time series and electron auto-correlation functions, is still at an early stage but all systems appear to have functioned correctly. What can be seen in data analyzed so far is a wide variety of electron responses to TX pulses, illustrated in Figure 45.

The nominally colored blocks, shown here in monochrome, on the left of Figure 45 correspond to plots of the superimposed time series summed over energy steps plotted against energy, while a few typical examples are shown as 2-D cuts on the right. At some energy - frequency combinations resonances decay slowly, while at others like the lowest 2-D cut there is a rapid decay with a response that closely mimics the TX pulse shape.

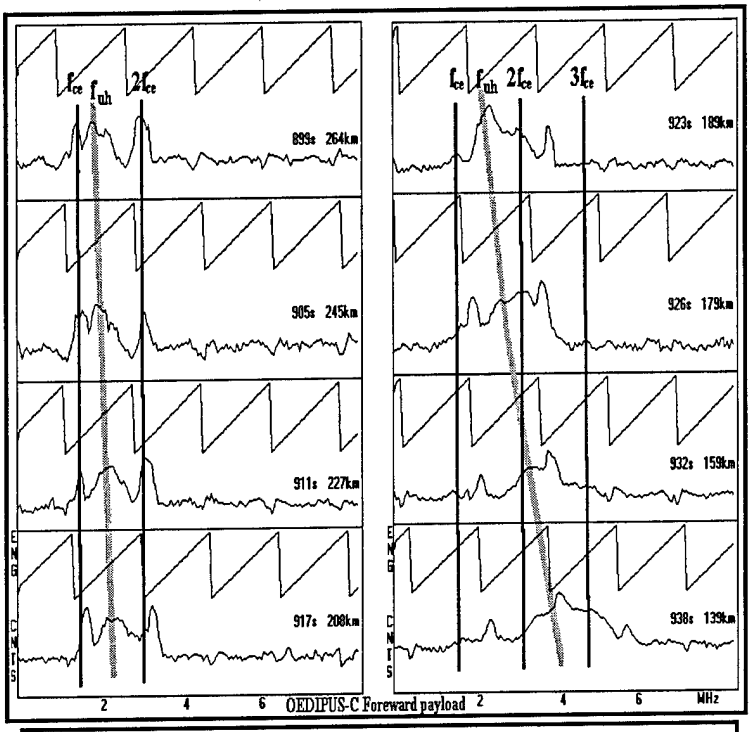

FIGURE 44: ELECTRON HEATING AS A FUNCTION OF TX FREQUENCY AFTER 899S. THE ENERGY SWEEP IS SHOWN FOR CLARITY

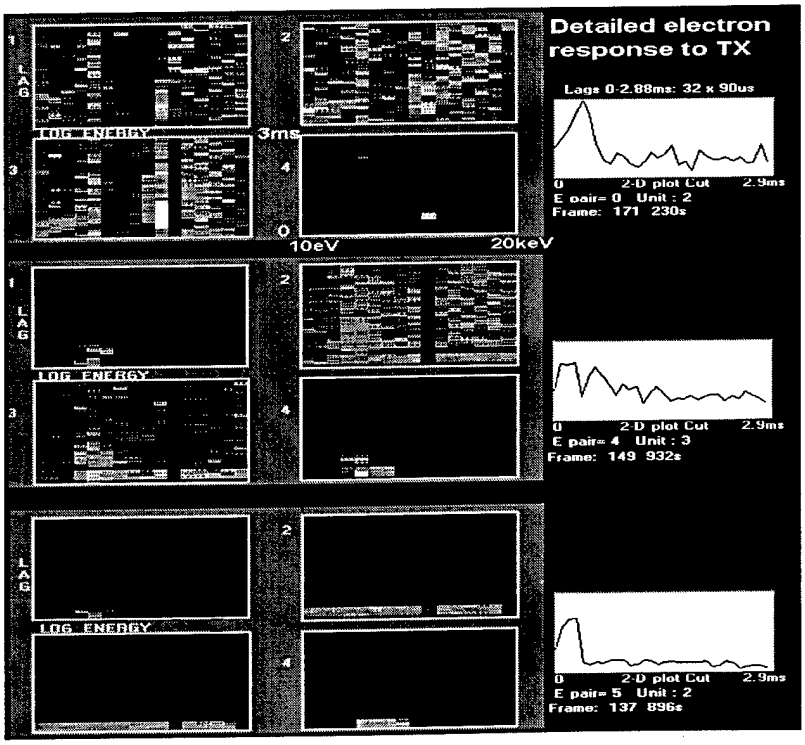

FIGURE 45: RESPONSE OF ELECTRONS TO TX PULSES IN HIGH RESOLUTION.

4.7 Summary

OEDIPUS-C systems performed well to meet the scientific objectives. All EPI systems, comprising some nine processing elements on each payload, operated without fault to produce a rich dataset on auroral wave-particle interactions, in particular, on-board EPI particle processing in both payloads provided direct measurements of electron heating, wave-particle interactions via particle correlators, and a high resolution measurement of wave induced particle heating via transmitter synchronised fast sampling. Strong electron heating was observed at times when the HF transmitter frequency was equal to a harmonic of the electron gyrofrequency, f_{ce}, or equal to the upper hybrid frequency, f_{uh}